Great Britain Journals Press

London Journal of Engineering Research
General Section

RESEARCH FINGERPRINT

IDENTIFIER
LJER-227759

PEER REVIEW
Double Blind

SIMILARITY CHECK
Perplexity AI and iThenticate

ACCESS
Open Access

LANGUAGE
English

PRINT ISSN
2631-8474

ONLINE ISSN
2631-8482

EDITION

ABBREVIATION
LJER

VOLUME
26

ISSUE
1

YEAR
2026

KEY DATES

RECEIVED
2026-05-11

ACCEPTED
2026-05-20

ONLINE PUBLISHED
2026-06-08

PUBLISHED
2026-06-24

CATALOGING

CROSSMARK DOI
10.34257/LJER227759UK

IEEE CLASS
4.1

UDC CLASS
621.45:629.7.03

ARXIV CLASS
physics.app-ph

ACM CLASS
J.2

ACCESS ONLINE

Article Record

Electro-Jet Engine: a Jet Engine without Turbine

CORRESPONDENCE

AUTHORS & AFFILIATIONS

Sorin NUTU ¶*

¶ National University of Science and Technology POLITEHNICA Bucharest, Bucharest, Ro

ABSTRACT

In accordance with efficiency criteria, the development of air transport has to the option of using large passenger airplanes, with capacities ranging from 200 to over 800 passengers and masses ranging from 100 to over 500 tons. These airplanes require a large airport infrastructure that involve major air security problems. The proposed idea is to use small, pressurized aircraft for passenger air transport, with a capacity of 4 to 9 people, including the crew, which can use small and minimally equipped airports, without complex security facilities, and can fly at altitudes of 12.000 to 18.000 m at supersonic speeds. These aircraft use Coanda-type jet engine, without a turbine, in which the compressor is driven by an electric motor, use hydrogen as fuel and are easily converted from a Coanda-type jet to a ramjet. This engine has devices for transforming thermal energy directly into...

Full abstract continues on the metadata continuation sheet.

Index Terms: electro-jet engine • Coanda-type jet engine • turbine-less • Seebeck bridge thermal-electric converters • hydrogen combustion • small passenger aircraft • operation from small airports • thermal-electric energy recovery

FUNDING
No external funding was declared for this work.

CONFLICTS
The authors declare no conflict of interest.

AI USAGE
No generative AI was used for analysis or results.

HOW TO CITE
NUTU (2026). Electro-Jet Engine: a Jet Engine without Turbine. London Journal of Engineering Research, 26(1), 13-35. DOI: 10.34257/LJER227759UK

METADATA CONTINUATION

AUTHOR CONTACT QR LEDGER

Sorin NUTU¶*

FULL ABSTRACT

In accordance with efficiency criteria, the development of air transport has to the option of using large passenger airplanes, with capacities ranging from 200 to over 800 passengers and masses ranging from 100 to over 500 tons. These airplanes require a large airport infrastructure that involve major air security problems. The proposed idea is to use small, pressurized aircraft for passenger air transport, with a capacity of 4 to 9 people, including the crew, which can use small and minimally equipped airports, without complex security facilities, and can fly at altitudes of 12.000 to 18.000 m at supersonic speeds. These aircraft use Coanda-type jet engine, without a turbine, in which the compressor is driven by an electric motor, use hydrogen as fuel and are easily converted from a Coanda-type jet to a ramjet. This engine has devices for transforming thermal energy directly into electrical energy, thus generating, in whole or in part, the electrical energy necessary to drive the compressor, until the conversion of the electro-jet engine into a ramjet engine. These proposals represent a new type of jet engine nevertheless a new concept in passenger air transport. Last part studies theoretically and experimentally the conversion of thermal energy directly into electrical energy. The experimental part was based on the recovery of a part of the heat lost to the cold source, i.e. to the atmosphere, through the walls of hot part of a turboshaft jet engine. For the experimental part I used a small turboshaft jet engine installed on an ultralight helicopter. The recovery was done with a Seebeck bridge currently produced. These Seebeck bridges are manufactured in mass production, have a low maximum operating temperature compared to the temperature inside the jet engine and have a very low efficiency compared to current systems used in space technology [21], [22].

ARCHIVAL RECORD

LJER · Vol 26 · Issue 1 · 2026

Article ID LJER-227759 · DOI 10.34257/LJER227759UK

Print ISSN 2631-8474 · Online ISSN 2631-8482

CROSSREF DOI 10.34257/LJER227759UK

RESEARCH ARTICLE

Electro-Jet Engine: a Jet Engine without Turbine

Sorin NUTU[¶*]

AFFILIATIONS

¶ National University of Science and Technology POLITEHNICA Bucharest, Bucharest, Ro

Abstract

In accordance with efficiency criteria, the development of air transport has to the option of using large passenger airplanes, with capacities ranging from 200 to over 800 passengers and masses ranging from 100 to over 500 tons. These airplanes require a large airport infrastructure that involve major air security problems. The proposed idea is to use small, pressurized aircraft for passenger air transport, with a capacity of 4 to 9 people, including the crew, which can use small and minimally equipped airports, without complex security facilities, and can fly at altitudes of 12.000 to 18.000 m at supersonic speeds. These aircraft use Coanda-type jet engine, without a turbine, in which the compressor is driven by an electric motor, use hydrogen as fuel and are easily converted from a Coanda-type jet to a ramjet. This engine has devices for transforming thermal energy directly into electrical energy, thus generating, in whole or in part, the electrical energy necessary to drive the compressor, until the conversion of the electro-jet engine into a ramjet engine. These proposals represent a new type of jet engine nevertheless a new concept in passenger air transport. Last part studies theoretically and experimentally the conversion of thermal energy directly into electrical energy. The experimental part was based on the recovery of a part of the heat lost to the cold source, i.e. to the atmosphere, through the walls of hot part of a turboshaft jet engine. For the experimental part I used a small turboshaft jet engine installed on an ultralight helicopter. The recovery was done with a Seebeck bridge currently produced. These Seebeck bridges are manufactured in mass production, have a low maximum operating temperature compared to the temperature inside the jet engine and have a very low efficiency compared to current systems used in space technology [21], [22].

Keywords: *electro-jet engine, Coanda-type jet engine, turbine-less, Seebeck bridge thermal-electric converters, hydrogen combustion, small passenger aircraft, operation from small airports, thermal-electric energy recovery*

Correspondence: Sorin NUTU

1 Introduction

The main idea is that a passenger airplane with a capacity of 4 to 9 seats **is no longer an interesting target for a hijacking**, in this case the security measures that are required in the case of an airplane with a large number of passengers are no longer necessary. This airplane, which would resemble a current business jet in terms of passenger capacity, is designed to be as efficient as possible, with reasonable comfort, and which can be flown according to current regulations with a single- or multi-pilot crew. If this airplane has the capacity to travel at speeds comparable to or higher than current airliners (Mach 2 to 4), even if not over long distances (long range), it will be an interesting alternative, considering also the possibility of operating from small airports or airfields with minimal ground equipment, using modern navigation systems (PBN-Performance Based Navigation, based on SBAS-Satellite Based Augmentation System) but also flying on RNAV-Area Navigation routes on demand, achievable under the current reorganization of the upper airspace.

If this airplane would be propelled by classic Whittle-type jet engines, the turbine would be very small, resulting in very high total losses. For this reason, it is necessary to replace the turbine with a set of an electric motor fed by a thermo-electric energy convertor. This airplane is equipped with an electro-jet engine, a Coanda-type jet engine with a compressor driven by an electric motor fed by Seebeck-type energy recovery bridges. For these devices, I will also present a study of systems that transform thermal energy directly into electrical energy. This airplane can use hydrogen as fuel and this **could be the non-polluting airplane of the future**. I present also an experiment for recovering the thermal energy lost through the jet engine walls that is a lost energy.

All of these above are contained in the patent application registered to Romanian Patent Office - OSIM under no. A/00293/24.07.2023, application made in my own name, as sole author.

Just to recall, the Coanda-type jet engine that equipped the airplane designed and built by the engineer with the same name, i.e. the Coanda-1910 airplane, exhibited at the "Second International Aeronautical Exhibition" at the "Grand Palais" in Paris, in October 1910, was a jet engine that was composed of a single-stage centrifugal compressor, driven by a piston engine, which had a fuel injection and combustion line on the ejected flow, and which took off accidentally on December 16, 1910, at Issy-les-Moulineaux, near Paris. We find it in the patents: with no.

416,541 of October 22, 1910, and in the appendix with no. 13,502 of April 29, 1911, to Paris, France; with no. 58,323 of May 26, 1911, to the Swiss Patent Office; with no. 12,740 of May 30, 1911 to British Patent; and with No. US 1,104,963 of July 28, 1914, registered in the United States of America.

This type of jet engine, called a motor-jet, can be found on the following airplanes equipped with it, in the year:

> - 1934: at the "Regia Aeronautica", on the Caproni-Campini N.1 (with the CC 2 coding) and Caproni CA-183bis aircraft;
> - 1938: at Heinkel, on the HeS50Z aircraft, the experimental version, and the HeS60 final version;
> - 1942: at the TSIAM Institute led by K.V. Khalshchevnikov, on the MiG-13 / I-250(N) aircraft, designed by the team led by the engineer Mikoyan and the mathematician Gurievich;
> - 1945: at Yokosuka Arsenal, the team led by engineers Tadano Mitsuzi and Masao Yamana, on the Yokosuka P1Y-1 "Ginga" bomber, on which the Coanda-type Tsu-11 jet engine was tested, and then the Yokosuka P1Y-3 "Ginga" Model 33 variant, carrier aircraft of the Okha11 kamikaze bomber, which was equipped, in one variant, creating the Okha22 model, also with the Tsu-11 jet engine. The Tsu-11 jet engine also equipped the Kikka aircraft, a high-speed, twin-jet fighter, as well as the Yokosuka MXY-9 "Shuka" training aircraft.

The advantages of this Coanda-type engine are:

> - no limitation of the maximum temperature in the cycle, thus facilitating the use of hydrogen as fuel and has a complete and efficient combustion of the fuel, not requiring extinguishing and cooling the flame after the combustion chamber at the turbine inlet;
> - simple conversion into a ramjet by rotating or retracting the rotor and stator blades of the compressor stages, if a multi-stage axial compressor is used.
>
> The disadvantages of the Coanda-type engine are:
> - limitation of the practical ceiling due to the decrease in piston engine power with altitude;
> - technological difficulties associated with the use of a less reliable piston engine;
> - the power, size and weight of the piston engine in accordance with aviation requirements lead to thrust limitations.

To eliminate the disadvantages of the classic Coanda-type jet engine, I replaced the piston engine that drives the compressor with an electric motor with a power similar to that of the piston engine and with a speed that is appropriate for driving an aviation compressor. I intend to use a multi-stage axial compressor, the centrifugal compressor being unsuitable for converting the jet engine from a classic jet to a ramjet. The electric motor is powered by an on-board battery and a set of Seebeck-type converters that transform thermal energy directly into electrical energy. The first part of the flight, i.e. take-off and climb to cruising altitude, will be based on energy generated by thermo-electric converters, but also on energy provided by the on-board battery. These on-board batteries have a higher capacity than those of a classic aircraft (they have a capacity of 2 to 3 times greater). Upon reaching cruising altitude or at altitudes that allow speeds at which dynamic compression is more efficient or comparable to mechanical compression in the axial compressor, the jet engine converts to a ramjet, by retracting or rotating the rotor and stator blades of the axial compressor stages. At this point, the Seebeck-type thermoelectric converters power the aircraft's electrical system and recharge the onboard batteries.

I mention the fact that it is possible to convert both the thermal energy from the gas flow after the combustion chamber, which is the useful energy of the jet engine, but it is also possible **to recover a part of the heat transferred through the hot parts of the engine to the outside**, which is **a part of the energy lost to the cold source $\mathbf{q_r}$** as I will estimate experimentally on the Part 2 of the article, estimating the degree of recovery of this energy.

Other **important advantage** of such a jet engine is, in addition to those listed above, the **much lower manufacturing and maintenance costs** compared to the classic turbojet variant, the Whittle-type, which requires both inspection and replacement after certain intervals of time of the "hot" part.

2 Applied Theory for the Study of the Electro-jet Engine

For the comparative study of this type of jet engine with a classic turbo-jet, I will make thermodynamic performance calculations.

I will start from the general equation of the thrust that appears in a static section of the engine, according to [1, 2, 3, 4, 5, 11].

$$\boldsymbol{F_{t\text{-}a}} = \iint_{S_2} \mathbf{v_2} d\dot{m}_2 - \iint_{S_1} \mathbf{v_1} d\dot{m}_1 + \iint_{S_1} p_1 \mathbf{n_1} dS_1 + \iint_{S_2} p_2 \mathbf{n_2} dS_2$$

For simplicity, I considered that the gas velocities in the inlet and outlet sections are subsonic, no shock waves appear, and thus the pressures in the inlet sections 1-1 and outlet 2-2 (Figure 1) do not have shock wave pressure jumps, meaning the internal and external pressures are equal, so:

$$p_{1\text{-}int} = p_{1\text{-}ext} = p_1 \; and \; p_{2\text{-}int} = p_{2\text{-}ext} = p_2$$

For the calculation of the estimated performances, I will make the following simplifying assumptions:

- the velocities $\boldsymbol{v_1}$ and $\boldsymbol{v_2}$ are constant in the inlet and outlet sections of the control volume, through the surfaces S_1 and S_2;
- the flow rates $\dot{m}_1$ and $\dot{m}_2$ are constant in the inlet and outlet sections of the control volume, through the surfaces S_1 and S_2;
- the flow duct is axially symmetrical, with the surfaces S_1 and S_2 perpendicular to the symmetry axis of the duct;
- the friction losses and thermal conduction losses through the walls of the flow duct are not taken into account;
- the flow is irrotational or potential and stationary or permanent;
- the thermodynamic constants k (adiabatic or isentropic exponent) and c_p (specific heat at constant pressure) are constant with temperature and equal between the inlet and outlet of the flow channels and have the value of those for air;
- the combustion is complete, at constant pressure, with the excess air coefficient equal to 1 (stoichiometric burn) and without dissociations;
- the composition of the working gas does not change before, during and after combustion;
- the contribution to thrust of the fuel flow and fuel enthalpy is neglected;
- the evolutions are isentropic;
- air is considered a perfect gas.

Starting from the integral equation above, respectively, the expression of the thrust in a closed channel, inside it, in absolute motion (i.e. in a static section of the engine), equation that will project onto the 0y axis, as shown in the drawing below (Figure 1).

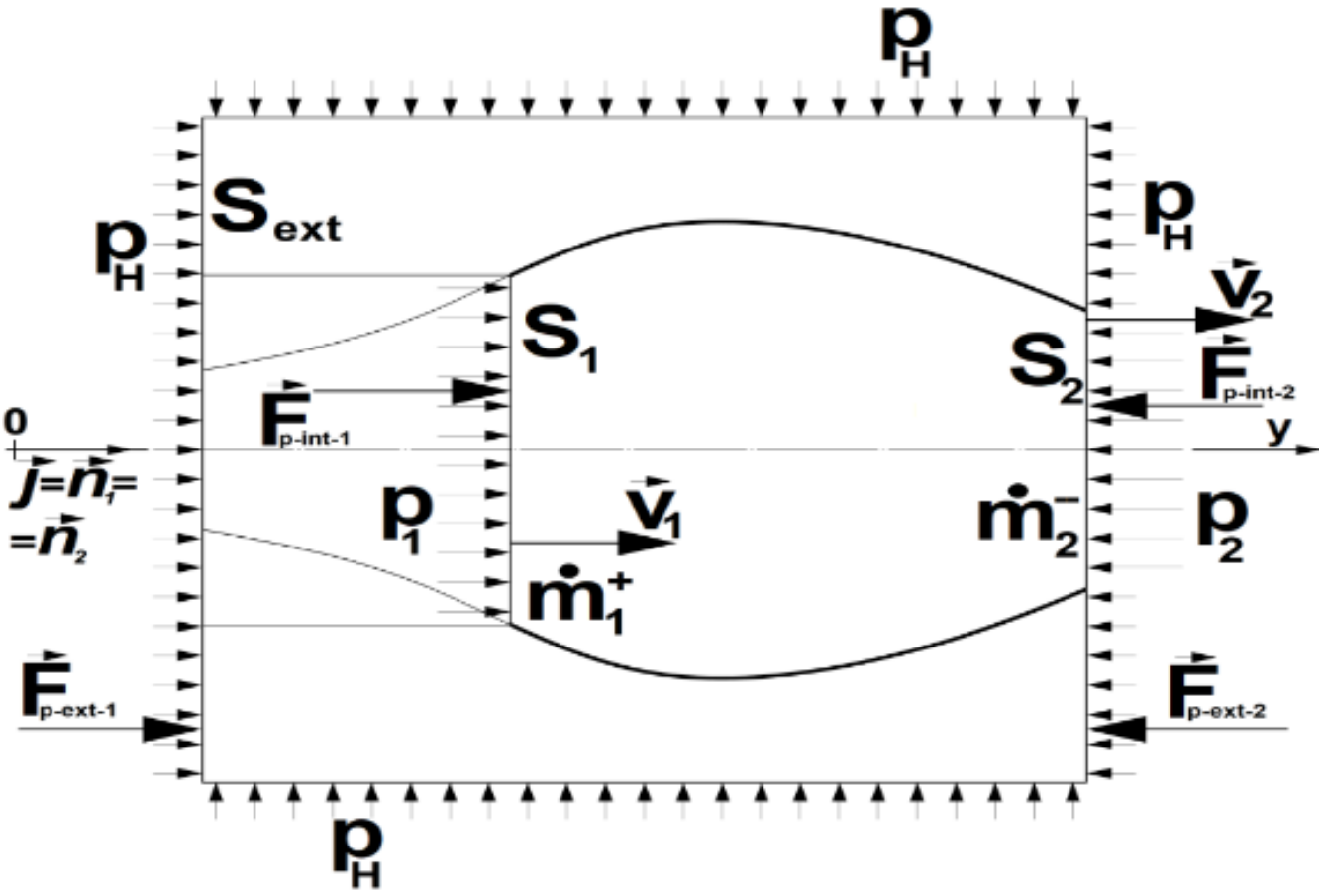

Figure 1. Jet engine or part of a jet engine thrust

In this case, we have the thrust of a pare of a jet engine part or of the jet engine as a whole, thrust that will have two components, namely, an internal component, defined in the equation below, denoted T_{int}, and an external component, resulting from the action of ambient pressure, p_H, which is distributed over a cylinder containing the flow section and extending radially into an undisturbed flow zone (for the whole jet engine) and is limited to the ends of the inlet and outlet sections of the flow channel to be studied.

It is observed that on the lateral surface of the control cylinder, the p_H pressures generate forces that cancel each other out, resulting in an external thrust T_{ext} as the sum of the pressure forces on the two ends of the cylinder. The thrust, in projection on the 0y axis is, as follows, according to [11]:

$$-T_{int} = -v_2\dot{m}_2 + v_1\dot{m}_1 - F_{p\text{-}int\text{-}2} + F_{p\text{-}int\text{-}1}$$

$$T_{int} = v_2\dot{m}_2 - v_1\dot{m}_1 + p_2S_2 - p_1S_1, \text{ si:}$$
$$-T_{ext} = -F_{p\text{-}ext\text{-}2} + F_{p\text{-}ext\text{-}1}$$
$$T_{ext} = (S_{ext} - S_2)p_H - (S_{ext} - S_1)p_H = S_{ext}p_H - S_2p_H - S_{ext}p_H + S_1p_H = -p_H(S_2 - S_1), \text{ so:}$$
$$T = T_{int} + T_{ext}, \text{ where:}$$
$$T = v_2\dot{m}_2 - v_1\dot{m}_1 + p_2S_2 - p_1S_1 - p_H(S_2 - S_1)$$

This thrust can be separated, according to [11], into two components, respectively, a momentum component T_R, and a pressure component T_P, that is:

$$T = T_R + T_P, \text{ where:}$$
$$T_R = v_2\dot{m}_2 - v_1\dot{m}_1 \text{ and:}$$
$$T_P = p_2S_2 - p_1S_1 - p_H(S_2 - S_1)$$

I will write, further, the thrust as a function of the relative parameters, defined between two sections, named section 1 defined as the inlet section, and section 2 defined as the outlet section. The speed will be highlighted by the parameter λ (called in some books also the Ceaplaghin number) that is the speed related to the speed in a critical section a_{cr} (more suitable for the jet engine, compared to the Mach number more suitable for the study of aircraft aerodynamics). I will also highlight the thermodynamic function of the momentum used in this chapter, starting from the definition of total enthalpy, respectively, according to [1, 7, 8]:

$$i^* = i + \frac{v^2}{2} \Rightarrow c_pT^* = c_pT + \frac{v^2}{2} \Rightarrow \frac{kR}{k-1}T^* = \frac{kR}{k-1}T + \frac{v^2}{2} \,/\cdot(k\text{-}1) \Rightarrow kRT^* = kRT + \frac{k-1}{2}v^2$$

where $kRT = a^2$, and a^2 is the speed of sound squared. And I'll have:

$$Z(\lambda) = \left(\lambda + \frac{1}{\lambda}\right), \text{ thermodynamic function of the momentum.}$$

With these notations, the thrust of the jet engine or a jet engine part can be written in the form:

$$T = v_2\dot{m}_2 - v_1\dot{m}_1 + p_2S_2 - p_1S_1 - p_H(S_2 - S_1), \text{ or:}$$
$$T = (v_2\dot{m}_2 + p_2S_2) - (v_1\dot{m}_1 + p_1S_1) - p_H(S_2 - S_1) = = \dot{m}_2a_{cr\text{-}2}\frac{k_2+1}{2k_2}Z(\lambda_2) - \dot{m}_1a_{cr\text{-}1}\frac{k_1+1}{2k_1}Z(\lambda_1) - p_H(S_2 - S_1) = \text{(where if I noted b} = \frac{k+1}{2k}\text{, I will have)} =$$
$$\dot{m}_1a_{cr\text{-}1}b_1Z(\lambda_1)\left[\frac{\dot{m}_2a_{cr-2}b_2Z(\lambda_2)}{\dot{m}_1a_{cr-1}b_1Z(\lambda_1)} - 1\right] - p_HS_1\left(\frac{S_2}{S_1} - 1\right) = \text{(where they will be noted with related quantities } \overline{X} \text{ between the inlet section: 1, and the}$$
outlet section: 2, respectively, $\overline{X} = \frac{X_2}{X_1}$, and $a_{cr} = \frac{a_{cr}}{a_0}a_0 = \sqrt{\frac{2}{k+1}kRT^*}$, where I noted $h = \sqrt{R\frac{k+1}{2k}}$, and then, according with [12]: $= \dot{m}_1h_1\sqrt{T_1^*}$
$$Z(\lambda_1)\left[\overline{\dot{m}h}Z(\lambda)\sqrt{\overline{T^*}} - 1\right] - p_HS_1(\overline{S} - 1),$$

or, I can define the specific thrust, respectively, the thrust related to the air flow through the inlet section: $T_{sp} = \frac{T}{\dot{m}_1}$, and I will have: $T_{sp} = h_1\sqrt{T_1^*}\,Z(\lambda_1)\left[\overline{\dot{m}h}Z(\lambda)\sqrt{\overline{T^*}} - 1\right] - \frac{p_HS_1}{\dot{m}_1}(\overline{S} - 1)$

$$T_{sp} = h_1\sqrt{T_1^*}\,Z(\lambda_1)\left[\overline{\dot{m}h}Z(\lambda)\sqrt{\overline{T^*}} - 1\right] - \frac{p_HS_1}{\rho_1S_1v_1}(\overline{S} - 1)$$
$$T_{sp} = h_1\sqrt{T_1^*}\,Z(\lambda_1)\left[\overline{\dot{m}h}Z(\lambda)\sqrt{\overline{T^*}} - 1\right] - \frac{p_H}{\rho_1v_1}(\overline{S} - 1)$$

In the case of a jet engine as a whole, the front of section 1-1 will appear as the flow tube at the air inlet in the undisturbed area. The specific fuel consumption of a jet engine as a whole will be: $C_{sp} = \dot{m}_c/T_{sp}$, where $\dot{m}_c$ is the fuel flow.

3 Comparison between Classic Turbo-jet Engine, Coanda-type Jet Engine and Electro-jet Engine

Particulary, I made a comparative study between a classic Whittle turbo-jet, in 6 compression ratio variants, with an axial compressor with 2, 3, and 4 stages, respectively, and a centrifugal compressor, with 1, 2, and 3 stages, respectively, a Coanda-type jet engine in the classic version (without energy recovery) as well as an electric-jet engine (with energy recovery, based on Seebeck bridges), in subvariants of classic fuel supply (kerosene), but also in subvariants of hydrogen supply.

For example, I will present such a calculation for a 2-stage centrifugal compressor, for the case of kerosene and hydrogen supply. In the first phase I will make a thermodynamic calculation in the ideal cycle, with the following assumptions, part of these stated above:

> - the component efficiencies in all variants and of the processes in the engines are 100%;
> - the gases evolutions are isentropic;
> - the coefficients c_p and k do not depend on the temperature, and have average, constant values, for the temperature range in which each variant operates. The air coefficient constant R has no variation with temperature;
> - during and after combustion, the working gas does not change its composition and the dissociation reactions during combustion are neglected;
> - combustion is done with an air intake excess coefficient λ=1 for the classic Coanda-type jet engine variants (motor-jet engine) and for the electro-jet engine;
> - for the classic turbo-jet, the maximum average temperature T_3^*, maximum in the cycle, of 2100K is considered, a temperature comparable to actual turbo-jets (source www.aviation.stackexchange.com);

- friction is neglected;
- heat losses through the engine walls are neglected;
- power losses spent by the jet engine aggregates and systems are neglected, with the exception of energy recuperators of the Seebeck-type bridge, which are considered to have a recovery efficiency of 100%;
- the mechanical compression work l_c does not depend on the aircraft speed (as a first approximation, especially for the axial compressor).

For the calculation of ideal cycles, the relationship used will be, according to [1, 9, 10]:

$$ds = c_p\frac{dT}{T} - R\frac{dp}{p} \;/\; \int_1^2 \Rightarrow s_2 - s_1 = c_p\ln\frac{T_2}{T_1} - R\ln\frac{p_2}{p_1} \Rightarrow s_2 - s_1 = c_p\ln\frac{i_2}{i_1} - R\ln\frac{p_2}{p_1} \Rightarrow s_2 = s_1 + c_p\ln\frac{i_2}{i_1} - R\ln\frac{p_2}{p_1} \quad (1)$$

and from (1):

$$i_2 = i_1\left(\frac{p_2}{p_1}\right)^{\frac{k-1}{k}}\left(\exp^{\frac{s_2-s_1}{c_p}}\right) \quad (1')$$

$$p_2 = p_1\left(\frac{i_2}{i_1}\right)^{\frac{k}{k-1}}\left(\exp^{-\frac{s_2-s_1}{R}}\right) \text{ where s is the enthropy} \quad (1'')$$

These equations are specific for the thermodynamic evolutions:

• Isothermic ($T_2 = T_1 \Rightarrow i_2 = i_1$) $s_2 = s_1 - R\ln\frac{p_2}{p_1}; \left(inverse\ p_2 = p_1\exp^{-\frac{s_2-s_1}{R}}\right)$ (2)

• Isobaric ($p_2 = p_1$) $s_2 - s_1 = c_p\ln\frac{i_2}{i_1} \Rightarrow \frac{s_2-s_1}{c_p} = \ln\frac{i_2}{i_1} \;/\cdot\exp \Rightarrow \exp^{\frac{s_2-s_1}{c_p}} = \exp^{\ln\frac{i_2}{i_1}} \Rightarrow \exp^{\frac{s_2-s_1}{c_p}} = \frac{i_2}{i_1} \Rightarrow i_2 = i_1\exp^{\frac{s_2-s_1}{c_p}}$

$\left(inverse\ s_2 = s_1 + c_p\ln\frac{i_2}{i_1}\right)$ (3)

• Isentropic ($s_2 = s_1$) $c_p\ln\frac{i_2}{i_1} = R\ln\frac{p_2}{p_1} \Rightarrow \ln\frac{i_2}{i_1} = \ln\left(\frac{p_2}{p_1}\right)^{\frac{R}{c_p}} \Rightarrow i_2 = i_1\left(\frac{p_2}{p_1}\right)^{\frac{R}{c_p}} \Rightarrow i_2 = i_1\left(\frac{p_2}{p_1}\right)^{\frac{k-1}{k}}$ $\left(inverse\ p_2 = p_1\left(\frac{i_2}{i_1}\right)^{\frac{k}{k-1}}\right)$ (4)

In these relations, I approximate, according to [9, 11], c_p=1083.2 J/kgK, k=1.3623, as constants with temperature (R=288.1 J/kgK being a constant with temperature and having the same value for air and combustion gases). For kerosene (Jet-A1) I have minL=14.598 kg Air/kg Kerosene, the stoichiometric quantity of air to burn chemically complete the fuel, the chemical energy of the fuel E_0=43150 kJ/kg, according to [9, 13] and Wikipedia. With these data I will have a maximum enthalpy increase after combustion, with an excess air supply λ=1:

$$\Delta i = E_0/(\text{minL Kerosene}) = 43150/14.598 = 2955.9 \text{ kJ/kg}$$

The value corresponds, according with [9, 13] for the adiabatic combustion temperature of kerosene under ISA-International Standard Atmosphere conditions which is 2455^0C / 2730K.

I will consider the possibility of using hydrogen as fuel, with a major consequence in reducing the carbon footprint and protecting the ozone layer at the tropopause altitude. While the development of aviation combustion chambers using pure hydrogen fuel—rather than mixtures with methane as discussed in [35, 36]—is still under academic and experimental investigation, the thermodynamic parameters can be estimated using established combustion models [14, 37]. Although detailed specifications for aircraft-level hydrogen storage and delivery systems remain proprietary or in early development stages, current research on cryogenic storage and hydrogen aviation timelines (e.g., studies by Airbus and NASA) suggests such technologies will be available in the near future, validating the thermodynamic assumptions of this work.

Related to this topic, I present below a variant for calculating the hydrogen combustion parameters, according to [6, 7, 9, 10, 35, 36, 37] as follows. The combustion reaction of H_2 (above I wrote the relative atomic masses of the components to the atomic mass of hydrogen which is considered to have an atomic mass equal to 1), will be:

$$\overset{(1)}{\widetilde{2H_2}} + \overset{(16)}{\widetilde{O_2}} = \overset{(18)}{\widetilde{2H_2O}}$$

$$\text{so: } 4\text{kgH}_2 + 32\text{kgO}_2 = 36\text{kgH}_2\text{O} \;/:4$$

$$1\text{kgH}_2 + 8\text{kgO}_2 = 9\text{kgH}_2\text{O}$$

But 8 kg of O_2 it is found in 8•4,292 kg of air, therefor:

1kgH_2 burn with minL=8•4,292 kgL=34,336 kgL/kgH_2

So: minL=34,336 kg Air/kg Hydrogen

From [12] we have for hydrogen, approximately, E0=120000 kJ/kg, which results in an energy released after combustion, found in the enthalpy increase, of:

$$\Delta i = E_0/\text{minL } H_2 = 120000/34.336 = 3494.9 \text{ kJ/kg}$$

The approximation k=1.3623, is also verified by taking into account the tables for the values of absolute temperature T, specific enthalpy i and specific entropy s for air at the standard pressure of 101325 Pa, as well as other information from [8] and [10].

I calculated the ideal cycle parameters in the variants and sub-variants presented above, in the first phase, under ISA-International Standard Atmosphere conditions, at sea level (MSL-Mean Sea Level or H=0 m) and at speed v=0 (at a fixed point, Table 1) and for altitude H=8000m and

speed M=0.8 (i.e. v=246.4m/s, Table 2). The calculations were performed with 5 significant digits. I started from ISA conditions at sea level, i.e. p_0=101325 Pa and t_0=15^{0}C=288.2K, with i_0=312.2 kJ/kg and s_0=6.8349 kJ/kgK, as average values between air and burnt gases, according to [10].

For the classic Coanda-type jet variant, I used a TAE Centurion 125-02-99 engine, with the following parameters (according to TCDS EASA E.055 of Continental Aerospace Technologies GmbH and POH Diamond DA40 D of Diamond Aircraft Industries GmbH):

- Maximum take-off power: 100kW/135HP;
- Jet-A1 fuel consumption, at take-off power: 29.1 l/h=23.4 kg/h.

For the electro-jet engine type I will use an axial compressor of PT6A turboprop jet engine [28] driven by a high-speed electric motor MGV950CAX type (source www.parker.com) with a power of 170kW and a speed of 20,000 rpm (the MGV860CBD type with a power of 94kW and the same speed could also be used), a motor produced by Parker Hannifin Manufacturing France SAS, a branch of the AC890 Drive Association. To generate electricity, I will use Seebeck bridges TEG2-50-50-40/200 type (source www.eureca.de), which produce 40W of energy each, have dimensions of 50x50 mm, weigh 38 grams and are produced by EURECA Messtechnik GmbH (2500 pcs. with a mass of 95 kg and a surface area of 6.25 m^2 for which a length of the hot part, at take-off thrust conditions, would result in a first approximation of 2200 mm; the combustion chamber and the diffuser being annular in shape with an outer diameter of 500 mm and an inner diameter of 400 mm). If the onboard batteries are used as an additional source of electrical energy for takeoff and climb to cruising altitude, then the electrical energy generation area can be reduced to half the estimated length, i.e. 1100 mm, and, accordingly, the mass of the Seebeck bridges is reduced to 48 kg. It is observed, in the case of the electro-jet engine, that there is an isobaric evolution 3*- 4*, where a quantity of energy is spent, which represents the energy that is recovered, with the Seebeck bridges, from the gas flow after the combustion chamber. This gas energy is directly converted into electrical energy, part of this energy is used for the electric motor that drives the compressor and the surplus energy is stored in an on-board battery (in case there is a deficit of electrical energy, for example, during the take-off, initial climb and cruising climb to cruising altitude, part of the energy stored in the on-board batteries can be used). Generally, when cruising, the aircraft reduces its power, depending on the chosen cruise, between 45% and 75% (usually it is reduced to approximately 50%), so the necessary power generated by the Seebeck bridges, taking into account the dynamic compression due to the cruising speed, is generally below 50% of the maximum power required for takeoff and climb to the cruising altitude. In the case of converting the electro-jet into a ramjet, at the cruising speed and altitude, the electric generators are used as on-board generators, which supply the aircraft's electrical system and also recharge the on-board batteries. It should be noted that a rigorous system-level power density (thrust-to-weight ratio) comparison of the entire electro-jet propulsion train (including the high-capacity batteries, electric motor, and Seebeck bridges) against a standard turbocompressor unit is highly dependent on the development of aerospace-grade components. The current weight estimates (e.g., 48 to 95 kg for the Seebeck bridges) are based on commercial-off-the-shelf (COTS) thermoelectric modules, which are not optimized for aviation power-to-weight ratios. In a fully realized aviation-grade system, lightweight high-performance thermoelectric materials (such as optimized half-Heusler or oxyselenide alloys) would be used, significantly reducing the deadweight penalty. Furthermore, at cruise speeds where the electro-jet functions primarily as a ramjet, the shaft-less architecture avoids the weight of a standard turbocompressor, and the thermoelectric system's role transitions from primary motor driving to supplying auxiliary on-board systems and battery recharging, mitigating the weight penalty of the electrical conversion system during the main flight phase.

I present the calculation results for a 2-stage centrifugal compressor, classic turbojet (TR figured) and Coanda-type jet, with the two sub-variants, classic Coanda jet (CC figured) and electro-jet (CR figured), which will have the following parameters (the power corresponding to the calculated air flow is P=100kW):

$$\pi_c^* = 9{,}0;\ l_c^* = i_0\left(\pi_c^{*\frac{k-1}{k}} - 1\right) = 247{,}8 \text{ kJ/kg} \Rightarrow \dot{m}_a = \frac{P}{l_c^*} = 0{,}40355 \text{ kg/s};$$

The calculation was made both for kerosene (Jet-A1, with the extension -K) and hydrogen (H_2, with the extension -H) fuel variants as well.

Table 1. Jet engine parameters at H=0 m, v=0 m/s

PARAM.	p [Pa]	T [K]	i [kJ/kg]	s [kJ/kgK]	Tsp [m/s]	Csp [kg/Nh]	Δ % Tsp	Δ % Csp
0=1*	101325	288.2	312.2	6.8349				
2*	911925	517.0	560.0	6.8349				
3* TR	911925	2100.0	2274.7	8.3532				
4* TR	591015	1871.2	2026.9	8.3532				
5 TR-K	101325	1170.6	1268.0	8.3532	1283.7	0.11765		
5 TR-H	101325	1170.6	1268.0	8.3532	1249.9	0.04195		
Dif.TR-K/H							**-2.6**	**-64.3**
3* CC/R-K	911925	3245.8	3515.9	8.8248				
3* CC/R-H	911925	3743.4	4054.9	8.9793				
5 CC-K	101325	1809.4	1959.9	8.8248	1884.9	0.13083	**46.8**	**11.2**
5 CC-H	101325	2086.7	2260.3	8.9793	1949.6	0.05378	**56.0**	**28.2**
Dif.CC-K/H							**3.4**	**-58.9**
4* CR-K	911925	2998.8	3268.1	8.7457				
4* CR-H	911925	3514.7	3807.1	8.9110				
5 CR-K	101325	1681.9	1821.8	8.7457	1817.3	0.13570	**41.6**	**15.3**
5 CR-H	101325	1959.2	2122.2	8.9110	1889.1	0.05550	**51.1**	**32.3**
Dif.CR-K/H							**4.0**	**-59.1**

Table 2. Jet engine parameters at H=8000 m, v=246.4 m/s

PARAM.	p [Pa]	T [K]	i [kJ/kg]	s [kJ/kgK]	Tsp [m/s]	Csp [kg/Nh]	Δ % Tsp	Δ % Csp
H	35650	236.1	255.7	6.9199				
1*	54352	264.1	286.1	6.9199				
2*	489182	473.8	513.2	6.9199				
3* TR	489182	2100.0	2274.7	8.5326				
4* TR	329385	1890.3	2047.6	8.5326				
5 TR-K	35650	1046.4	1133.5	8.5326	1164.0	0.13328		
5 TR-H	35650	1046.4	1133.5	8.5326	1126.0	0.04784		
Dif.TR-K/H							**-3.3**	**-64.1**
3* CC/R-K	489182	3202.6	3469.1	8.9898				
3* CC/R-H	489182	3700.2	4008.1	9.1462				
5 CC-K	35650	1595.9	1728.7	8.9898	1747.1	0.14115	**50.1**	**5.9**
5 CC-H	35650	1843.8	1997.2	9.1462	1817.4	0.05769	**61.4**	**20.6**
Dif.CC-K/H							**4.0**	**-59.2**
4* CR-K	489182	2993.0	3242.0	8.9164				
4* CR-H	489182	3490.6	3781.0	9.0830				
5 CR-K	35650	1491.4	1615.5	8.9164	1680.8	0.14672	**44.4**	**10.1**
5 CR-H	35650	1739.4	1884.1	9.0830	1758.1	0.05964	**56.1**	**24.7**
Dif.CR-K/H							**4.6**	**-59.3**

With these calculated data, the i-s diagrams are drawn for the three variants with one, respectively, with two sub-variants (I mention that these variants were drawn to scale, Figures 2, 3 and 4):

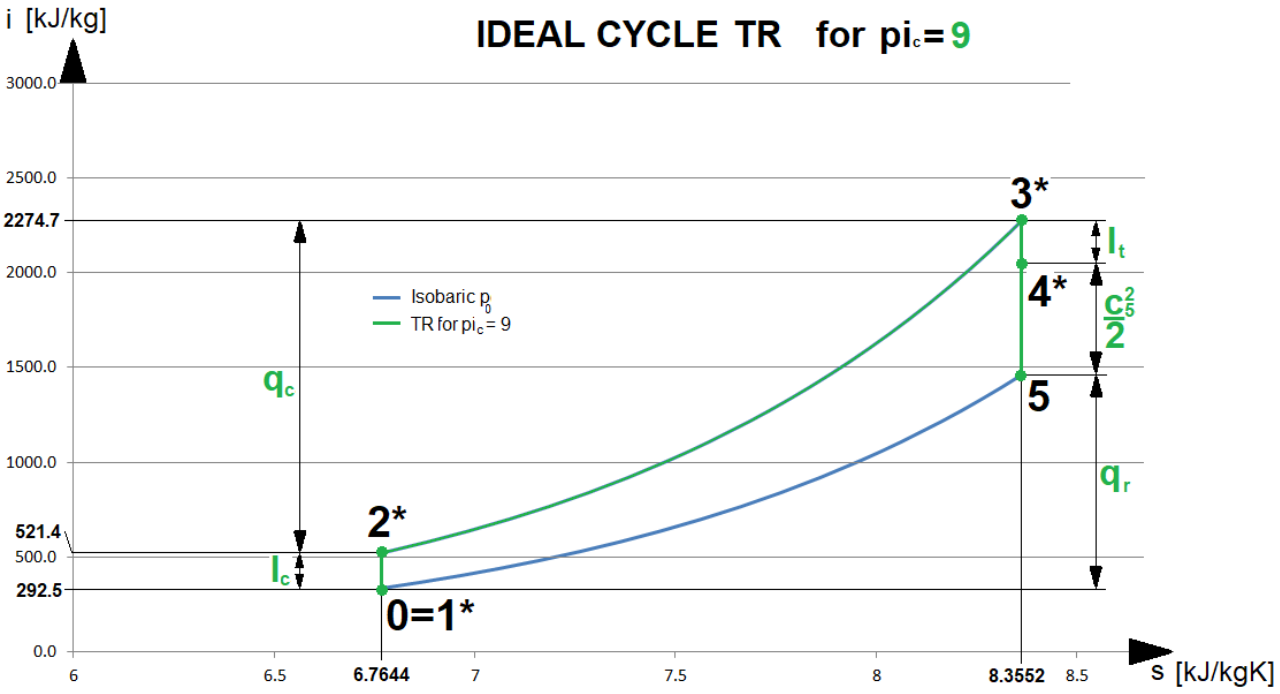

Figure 2. Ideal cycle for turbo-jet engine

In the case of the Coanda-type jet, in the classical and electric versions the relationship between the mechanical compression work l_c and the power P of the piston engine or electric motor is: $P=l_c \cdot \dot{m}_a$, where $\dot{m}_a$ is the air flow of the compressor.

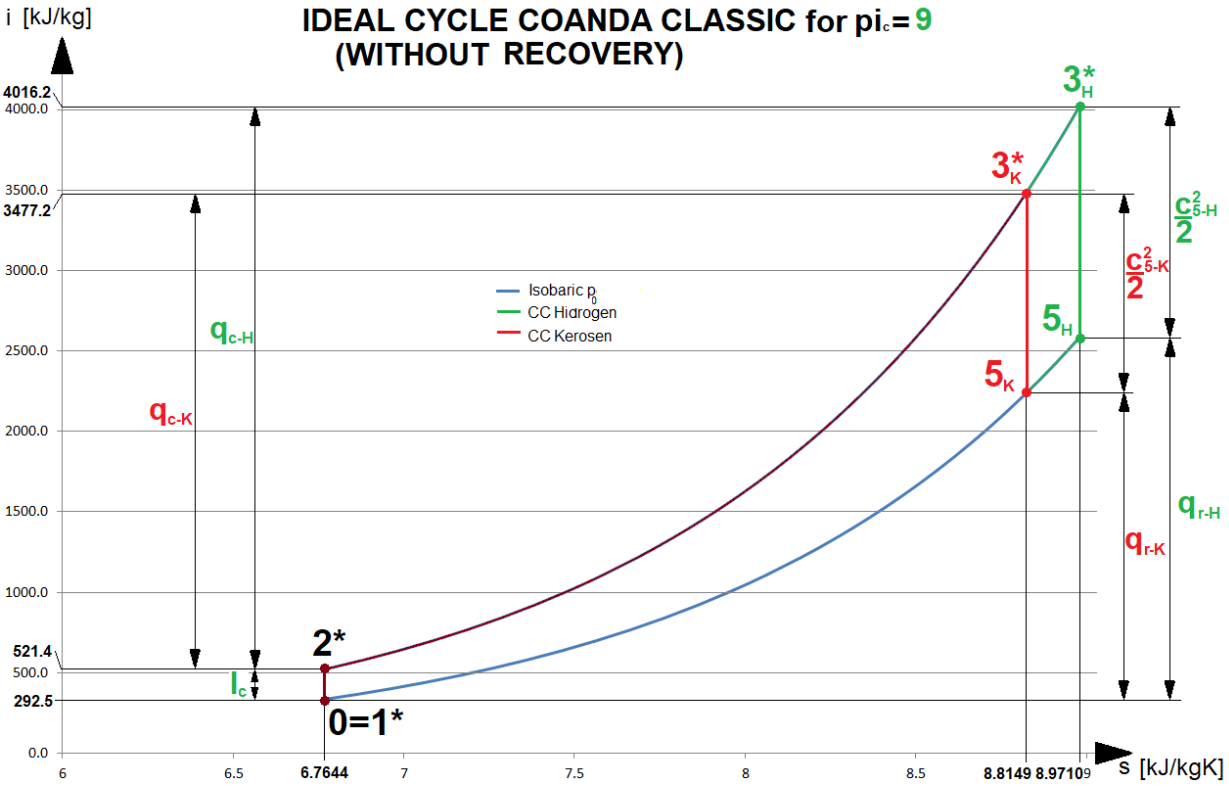

Figure 3. Ideal cycle for Coanda-type jet engine

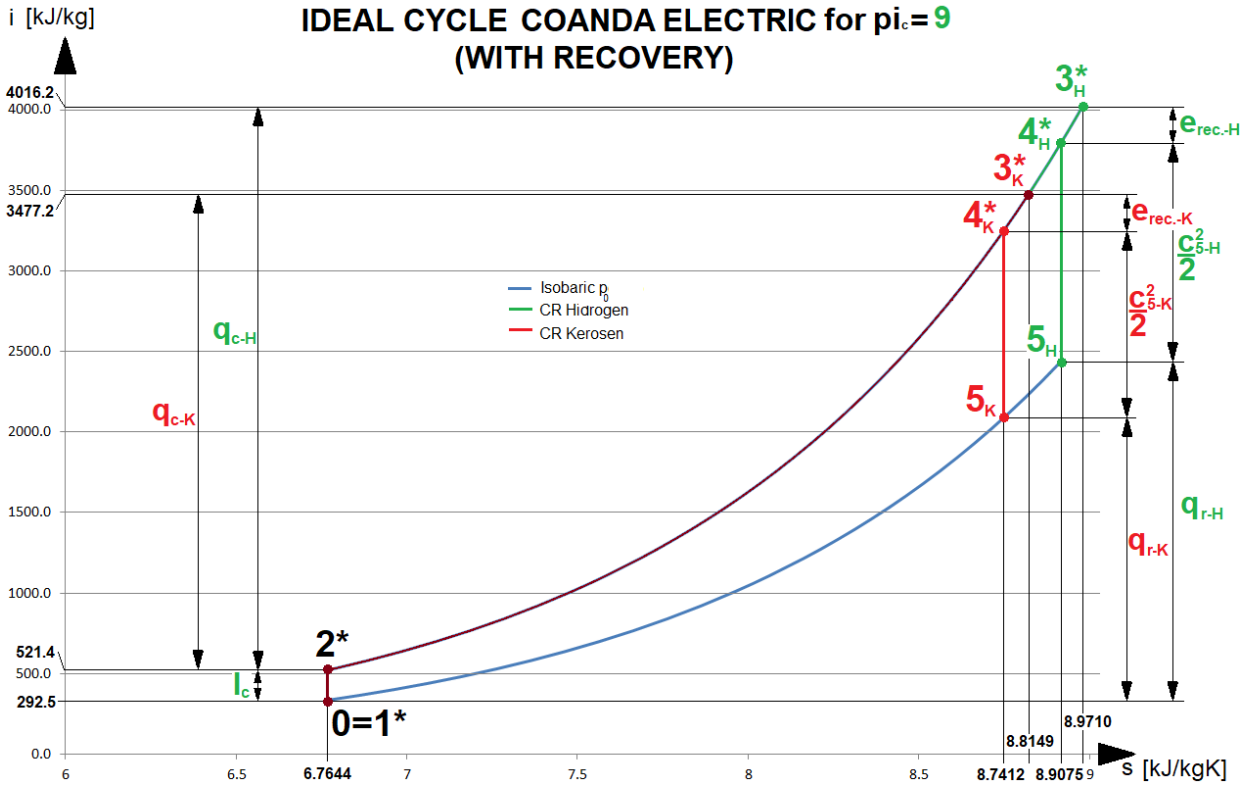

Figure 4. Ideal cycle for electro-jet engine (recovery jet engine)

To be closer to reality, I will also do a check in the real cycle, for MSL and fixed-point variants, and for the calculation of the real cycle I will use the thermodynamic tables from [10] but also information about the thermodynamic parameters of some combustible substances, such as kerosene and hydrogen, from [6] and [8]. I will also consider the dissociation during combustion for the first equilibrium.

Thus, for the calculation of the composition of the burnt gases in the case of kerosene (or Jet-A1 fuel), according to [10], I can consider a mass participation of the standard fuel (for simplification) as follows:

c=0.8608 kg C/kg fuel; h=0.1392 kg H/kg fuel,

and for a mass composition of air (considering, for simplification, that it has a volumetric composition of 79% N_2 and 21% O_2, where the percentage of approximately 1% Ar was added to nitrogen which is an inert gas, and the rest of the components, which are below 0.1%, will be neglected) of approximately (we symbolize air with L):

4.292 kg L/kg O2 (and, respectively, 3.292 kg N2/kg O2)

In this case, I have:

minL kg=4.292(8/3c + 8h) kg L/kg fuel=14.632 kg L/kg fuel for stoichiometric conditions

If kerosene is considered as a hydrocarbon compound with a conventional chemical formula of the form $C_{12}H_{23}$ as defined in [14], from which a mass participation results as:

c=0.8623 kg C/kg fuel; h=0.1377 kg H/kg fuel, which results in a value minL=14.598 kg L/kg fuel, values that are close to the values above and I will use in the future.

For the calculation of the combustion temperature, information from [6, 8] and [10] will be used, as follows:

- the energy balance of the combustion will be, according to [8]:

$$\dot{m}_c i_{comb.\text{-}Tini.} + \dot{m}_a i_{aer\text{-}Tini.} + \dot{m}_c E_0 = \dot{m}_g i_{g.a.\text{-}Tini.} + \dot{m}_c (Q_p)_{Tini.} = \dot{m}_g i_{g.a.\text{-}Tfin.} \text{ where:}$$

$$\dot{m}_a/\dot{m}_c = \lambda minL \text{ si } \dot{m}_g = \dot{m}_a + \dot{m}_c \text{ and I have:}$$

$$i_{comb.\text{-}Tini.} + \lambda minL i_{aer\text{-}Tini.} + E_0 = (1+\lambda minL) i_{g.a.\text{-}Tini.} + (Q_p)_{Tini.} = (1+\lambda minL) i_{g.a.\text{-}Tfin.}$$

where:

- i is the enthalpy of the fuel, air or burnt gases at the initial and final temperatures, respectively;
- E_0 is the chemical energy of the fuel (sometimes it can be defined as the lower or upper calorific value Pci or Pcs);
- $(Q_p)T$ is the heat of reaction, at constant pressure, and at a certain temperature.

These last two quantities can be taken from thermodynamic tables, or can be calculated approximately, according to [8]:

$(Q_p)_{C\alpha H\beta\text{-}T} \approx 393777\alpha + 241989(\beta/2)$ kJ/kmol and:

$P_{ci} \approx 32814c + 120995h$ kJ/kg.

If the enthalpy of the initial substances is considered to be $i_{s.i.\text{-}Tini.} = i_{comb.\text{-}Tini.} + \lambda \min L i_{aer\text{-}Tini.}$ and the enthalpy of the final substances $i_{s.f.\text{-}T} = (1+\lambda \min L) i_{g.a.\text{-}T}$ at the initial and final temperatures, respectively, the energy balance will become (in all these cases the heat of formation of the component substances is neglected):

$$i_{s.i.\text{-}Tini.} + E_0 = i_{s.f.\text{-}Tini.} + (Q_p)_{Tini.} = i_{s.f.\text{-}Tfin.}$$

where I have, formally, two evolutions (equivalent to the chemical reaction of fuel combustion), respectively, a first transformation of isothermal input of chemical energy of the fuel E_0 at temperature $T_{ini.}$, followed by a transformation of isobaric input of reaction energy at constant pressure Q_p, between the initial temperature $T_{ini.}$ and the final temperature $T_{fin.}$.

I will consider the values for these quantities, for kerosene, from tables in [6, 8] and [10] as follows:

$E_0 = 43150$ kJ/kg, $(Q_p)_{500K} = 7039050$ kJ/kmol.

In the case of hydrogen, I mention again that I did not found sufficient documentation for the combustion parameters, finding only the following data presented by Alejandro Millán-Merino and Pierre Boivin [14]:

- according to [11] $(Q_p)_{500K} = 243642$ kJ/kmol si $(Q_p)_{550K} = 244111$ kJ/kmol;
- according to [7] $P_{ci} = 119617$ kJ/kg, $P_{cs} = 141974$ kJ/kg = 242071 kJ/kmol,

$Q_p = 241746$ kJ/kmol = 119910 kJ/kg (water vapor, T not defined),

$Q_p = 285791$ kJ/kmol = 59491 kJ/kg (liquid water, T not defined),

$R = 412$ J/kgK, $\mu = 2{,}016$ kg/kmol, $\min O_2 = 8$ kg O_2/kg H_2,

$\min L = 34{,}336$ kgL/kg H_2.

I will consider $E_0 = 120000$ kJ/kg, $(Q_p)_{500K} = 238642$ kJ/kmol si $(Q_p)_{550K} = 240111$ kJ/kmol, $R = 412$ J/kgK, $\mu = 2{,}016$ kg/kmol that is the kmol mass, $\min L = 34{,}336$ kgL/kg H_2.

For a most accurate calculation of the combustion temperature, I will also consider the dissociation reactions, taking into account the first dissociation equilibrium, both for kerosene and for hydrogen. According to [8] and [10], in the case of dissociation, I have an equilibrium for the components before and after dissociation, of the form:

$$qA + rB + \ldots \leftrightarrow sC + tD + \ldots$$

where: $\overrightarrow{W_1} = k_1 \bullet p_A^q \bullet\ p_B^r \bullet \ldots$ is the reaction speed of the initial gas substances, that has p_A, p_B, ... are partial pressure for initial gases, and $\overleftarrow{W_2} = k_2 \bullet p_C^s \bullet\ p_D^t \bullet \ldots$ is the reaction speed of the final gas substances, that has p_C, p_D, ... are partial pressure for initial gases, and $\overrightarrow{W_1} = \overleftarrow{W_2}$, where k_1 and k_2 are the reaction constants.

The equilibrium equation can be written in the form:

$$K_p = \frac{k_1}{k_2} = \frac{p_C^s \bullet\ p_D^t \bullet \ldots}{p_A^q \bullet\ p_B^r \bullet \ldots}$$

where K_p is an equilibrium constant.

From the properties of the gas mixture, according to [10] we have:

$p_{am} = \sum_{i=1}^{n} p_i$, where $p_i = r_i p_{am}$, where $r_i = V_i/V$ is the volume participation of gases in the mixture, and p_i is the partial pressure of gases in the mixture, and:

$$V = \sum_{i=1}^{n} V_i \,,\ \sum_{i=1}^{n} r_i = 1$$

and

$$r_i = \frac{\frac{m_i}{\mu_i}}{\sum_{i=1}^{n} \frac{m_i}{\mu_i}} = \frac{\nu_i}{\nu_{am}}$$

where $\nu_{am} = \sum_{i=1}^{n} \frac{m_i}{\mu_i}$, ν_i is the kmol quantity of i component, and μ_i is the kmol mass of i component.

From here we have:

$$p_i = \frac{\nu_i}{\nu_{am}}\, p_{am}$$

Under these conditions, I will have:

$$K_p = \left(\frac{p_{am}}{\nu_{am}}\right)^{(s+t+\ldots)-(q+r+\ldots)} \frac{\nu_C^s \bullet \nu_D^t \bullet \ldots}{\nu_A^q \bullet \nu_B^r \bullet \ldots}$$

I will consider the first equilibrium, which is as follows:

- for kerosene: carbon monoxide equilibrium: $CO + 1/2O_2 \leftrightarrow CO_2$;
- for hydrogen: hydrogen equilibrium [14]: $H_2 + 1/2O_2 \leftrightarrow H_2O$.

From an energetic point of view, in the case of considering dissociations, the energy balance is:

$$i_{s.i.\text{-}Tini.} + E_0 = i_{s.f.\text{-}Tini.} + (Q_p)_{Tini.} = i_{s.f.\text{-}Tfin.\text{-}disoc.} + E_{0\text{-}disoc}$$

where: $E_{0\text{-}disoc.}$ is the energy lost due to dissociation reactions that will be subtracted from the enthalpy of the final substances at the final temperature $i_{s.f.\text{-}Tfin.} = i_{s.f.\text{-}Tfin.\text{-}disoc.} + E_{0\text{-}disoc.}$, which means a decrease in enthalpy, respectively a decrease of the final temperature after combustion.

To estimate the losses in the jet engine, I took information from [8] and [13], as follows:

- $\sigma_{DA}^{*} = 0,98$ total pressure losses in the intake device;
- $\eta_{C}^{*} = 0,75$ compressor efficiency;
- $\sigma_{CA}^{*} = 0,95$ total pressure losses in the combustion chamber;
- $\xi_{CA} = 0,95$ combustion chamber perfection coefficient;
- $\eta_{T}^{*} = 0,90$ turbine efficiency;
- $\eta_{M} = 0,99$ mechanical efficiency;
- $\varphi_{AR} = 0,97$ losses in the jet nozzle.

The calculation of the real cycles was made for ISA conditions ($T_0 = 288.16K$, $p_0 = 101325Pa$), at H = 0m and v = 0m/s. The calculations were made using the thermodynamic tables from [10]. Kerosene (Jet A1 fuel) will be taken into account defined as the approximate chemical formula $C_{12}H_{23}$, according to [13] (Table 3). The interpolations between the intermediate values in the tables are linear interpolations. I will consider $R_{air} = 0.2882$ kJ / kgK, $k_{air\text{-}average} = 1.39$ (constant between 300K and 550K). I chose $\pi_{c}^{*} = 9.00$ and, for TR (classic turbojet), T3 * = 2100K. For Coanda-type jets, both variants, classic and electric, I consider $\lambda = 1.05$, taking into account the secondary flow through the combustion chamber to protect its walls. Calculations were made with 5 significant digits with rounding.

Table 3. Real cycle parameters for jet engines

Param.	**p**	**T**	**i**	**s**	**Tsp**	**Csp**	**lc***
↓POINT	[Pa]	[K]	[kJ/kg]	[kJ/kgK]	[m/s]	[kg/Nh]	[kJ/kg]
0	101325	288.2	287.1	6.8210	-	-	-
1*	99299	288.2	287.1	6.8268	-	-	-
2*id	893687	540.0	537.9	6.8268	-	-	250.77
2*	893687	584.3	582.1	6.8486	-	-	295.02
3* TR-K	849003	2100.0	2567.5	8.4594	-	-	-
4* TR-Kid	471482	1826.4	2236.4	8.4594	-	-	-
4* TR-K	471482	1850.0	2269.5	8.4776	-	-	-
5 TR-Kid	101325	1322.1	1544.1	8.4776	1204.5	-	-
5 TR-K	101325	1379.0	1586.9	8.4982	1224.9	0.1422	-
3* TR-H	849003	2100.0	2815.1	9.2581	-	-	-
4* TR-Hid	504603	1882.8	2484.0	9.2581	-	-	-
4* TR-H	504603	1904.7	2517.1	9.2763	-	-	-
5 TR-Hid	101325	1344.8	1692.1	9.2763	1284.5	-	-
5 TR-H	101325	1379.8	1740.8	9.3076	1268.5	0.0513	-
3* CC/R-K	849003	2504.2	3133.7	8.7060	-	-	-
5 CC-Kid	101325	1607.7	1894.3	8.7060	1574.4	-	-
5 CC-K	101325	1459.3	1967.5	9.8970	1626.8	0.1444	-
3* CC/R-H	849003	2645.5	3963.7	10.1443	-	-	-
5 CC-Hid	101325	1729.3	2422.3	10.1443	1755.8	-	-
5 CC-H	101325	1789.0	2513.4	10.1738	1750.3	0.0570	**e-rec***
4* CR-K	849003	2239.1	2761.2	8.5487	-	-	372.5
5 CR-Kid	101325	1428.7	1655.9	8.5487	1486.8	-	-
5 CR-K	101325	1297.8	1721.2	9.7178	1536.3	0.1529	-
4* CR-H	849003	2428.9	3591.2	9.9970	-	-	372.5
5 CR-Hid	101325	1578.0	2179.1	9.9970	1680.5	-	-
5 CR-H	101325	1633.6	2262.6	10.0270	1675.3	0.0596	-

4 Conclusions

As a conclusion of the comparative theoretical study, on ideal cycle, for various heights and speeds, and between the ideal cycle and the real cycle on the ground and at a fixed point, it results:

- on the ground and at a fixed point, the electro-jet engine has an increase of 41.6% in specific thrust compared to the Whittle-type turbo-jet engine, with an increase in specific fuel consumption of 15.3% if kerosene is used as fuel, and an increase of 51.1% in thrust and of 32.3% in specific fuel consumption if hydrogen is used as fuel;

- at 8000 m and at M 0.8 (246.4 m/s = 887 km/h = 479 kts) the increase in specific thrust of the electro-jet engine is 44.4% with an increase of the specific fuel consumption of 10.1% compared to the Whittle-type turbo-jet engine if kerosene is used as fuel, and a 56.1% increase in specific thrust with a 24.1% increase in specific fuel consumption, if hydrogen is used as fuel. This estimation was made on the ideal cycle for both jet engine variants.

For the calculation on the real cycle, taking into account the first equilibrium for the combustion with dissociation, on the ground and at a fixed point, the increase in thrust for the electro-jet engine, compared to the turbo-jet engine is of 25.4% for the specific thrust and of 7.5% for the specific fuel consumption, when using kerosene as fuel and of 32.1% for the specific thrust and a 16.2% increase in the specific fuel consumption, when using hydrogen as fuel.

I mention that I made this calculation taking into account the recovery of thermal energy from the main flow of exhaust gases for the generation of electrical energy with Seebeck bridges. I mention that in chapter 8, I make an experimental estimation of the recovery of the energy lost through the hot parts of a small turbo-shaft jet engine, energy that constitutes an irretrievable loss in a conventional turbojet.

5 Types of Thermo-Electric Generators That Could Be Used for Electro-Jet Engine

I will present, without limiting myself to these, several types of thermoelectric generators that could be used to convert thermal energy in the form of heat directly into electrical energy, according to [15].

5.1 Thermo-electronic generator

A thermo-electronic generator is based on the emission of electrons from a cathode heated to a sufficiently high temperature to set the conduction electrons in motion. Such a generator is based on Richardson's theory of electron emission (Figure 5).

The Richardson formula is:

$$j = BT^2 \exp^{-\frac{\varphi}{kT}}$$

where:

j → current density in A/cm^2;
B → a constant = 120 A/(cm^{2}K^2);
T → absolute temperature in K;
φ → work of extraction of the electron in eV;
k → Boltzmann constant = 8,62·10^{-5} eV/K.

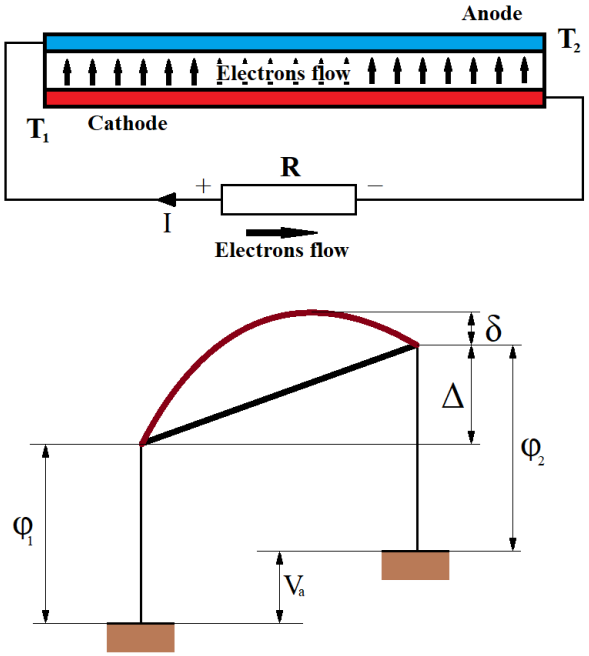

Figure 5. Thermo-electronic generator layout and energy levels of the generator

The thermo-electronic generator could be used in the combustion chamber area, when using materials that can withstand high temperatures, such as tungsten (or wolfram). The technical condition that determines the use of this method is the very small gap between the anode and cathode, the electrodes generating electro-motor voltage, of the order of tenths or hundredths of a millimeter, but also maintaining the vacuum between the anode and cathode that is a technical difficulty.

5.2 Magneto-hydro-dynamic (mhd) generator

The Magneto-hydro-dynamic generator is based on the Lorentz theory, in such a sense that in a magnetic field $\boldsymbol{B}$, in which an ionized gas moves with a velocity $\boldsymbol{v}$, an electromotive force (E.M.F.) $\boldsymbol{E}$ is generated between two plates connected to a load resistance R_{load} (Figure 6).

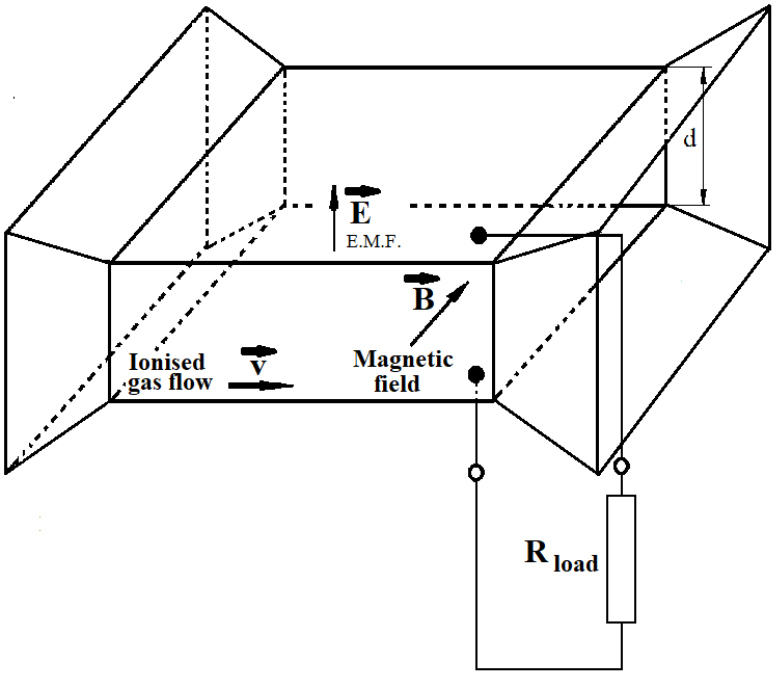

Figure 6. Magneto-hydro-dynamic generator layout

According to Lorentz's theory, the force generated by the electric charge q moving with a velocity $\boldsymbol{v}$ in the magnetic field of intensity $\boldsymbol{B}$ is:

$$\boldsymbol{F}_{Lorentz} = q(\boldsymbol{v}\text{x}\boldsymbol{B})$$

In this first case, the Lorentz force is

$$\boldsymbol{F} = q(\boldsymbol{E}+\boldsymbol{v}\text{x}\boldsymbol{B})$$

where $\boldsymbol{E}$ is the electric field existing in the working gas flow area (Figure 7).

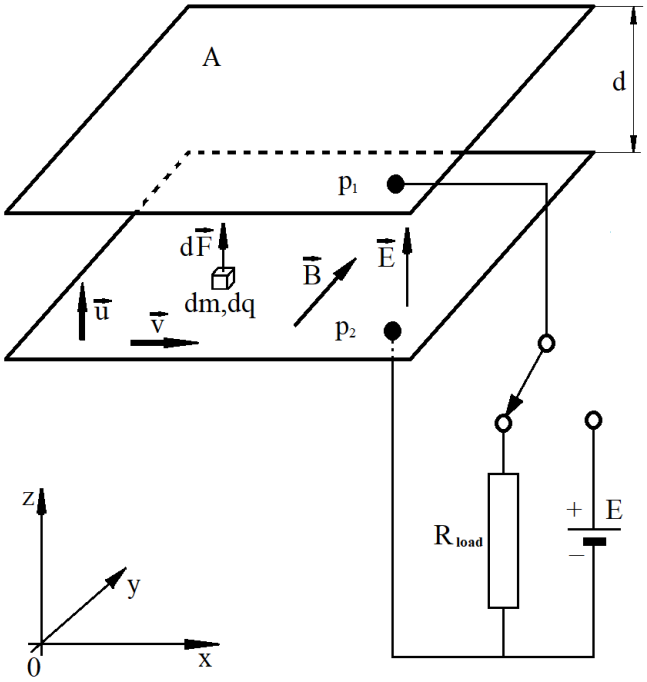

Figure 7. Magneto-hydro-dynamic generator equilibrium

But because of the electric field $\boldsymbol{E}$ generated by the electric potential difference U between plates p_1 and p_2, an electromagnetic force appears that causes the ionized working gas particle move at velocity $\boldsymbol{u}$, from p_2 to p_1.

So, finally, the force $\boldsymbol{F}$ acting on the ionized working gas particle, moving in the generation zone (between plates p_1 and p_2) is:

$$\boldsymbol{F} = q(\boldsymbol{E} + \boldsymbol{v}\text{x}\boldsymbol{B} + \boldsymbol{u}\text{x}\boldsymbol{B})$$

where $\boldsymbol{u}$ is the velocity of movement of the particle from plate p_2 to plate p_1, and:
$E = \frac{U}{d}$, where U is the potential difference between plates p_1 and p_2 and d is the distance between them.
In this case:

$$U_{total} = U + B \cdot v$$

where $B \cdot v = U_0$ is the open-circuit e.m.f. (considering also that vectors $\boldsymbol{v}$ and $\boldsymbol{u}$ are perpendicular to vector $\boldsymbol{B}$).

The magneto-hydro-dynamic generator would be suitable for use, but due to the need to use a strong magnetic field (which can be generated by powerful electromagnets, which are heavy and require high electrical power) and the need to ionize the exhaust gases, which is done by spraying ionizing elements (such as potassium or cesium powder) which would be a polluting and very expensive material, it is not feasible for use in aviation for this type of jet engine.

5.3 Seebeck thermo-electric generator (teg)

The Seebeck thermoelectric generator is based on the appearance of a potential difference between two conductors of different materials welded together. This phenomenon is called the thermoelectric effect or Seebeck effect.

The generator is composed of two welds between two such materials, one of the welds being placed in the hot source and the other being placed in the cold source (Figure 8).

The Seebeck electromotive force, as a potential difference is: $\Delta E = \alpha \Delta T \,/\, \cdot d \Rightarrow dE = \alpha dT, \{E_1 - E_2 = \alpha(T_1 - T_2)\}$

The coefficient α, in some books is called the thermal force and is measured in [V/K].

The energy transformed from the form of heat is: $Q = \Phi \cdot I \cdot t$, where Φ is called the Peltier coefficient, $\Phi = \alpha T \Rightarrow Q = \alpha T I t$, t is time and where:

Received heat : $Q_1^{rec.} = \alpha T_1 I t$: from hot source;

Disposed heat : $Q_2^{dis.} = \alpha T_2 I t$: from cold source;

And work is : $L = \alpha(T_1 - T_2) I t = Q_1^{rec.} - Q_2^{dis.}$.

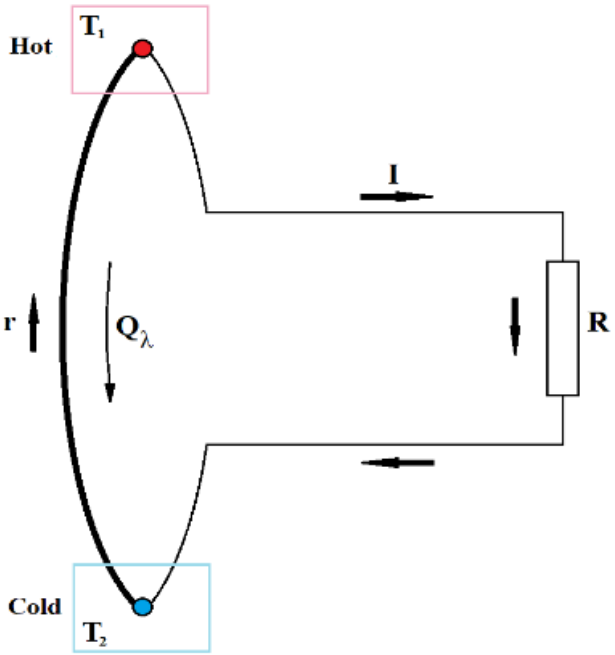

Figure 8. Seebeck generator layout

In this case the work L is:

$$L = Q_{Joule} + L_{cycle} = \alpha(T_1 - T_2) I t \Rightarrow L_{cycle} = \alpha(T_1 - T_2) I t - Q_{Joule} = I^2 R t$$

and the generated power is:

$$P = I^2 R = \alpha(T_1 - T_2) I$$

If $Q_\lambda^{conduction}$ is the heat exchanged by conduction between the hot source and the cold source, and Q_{Joule} is the heat released by the thermo-electric Joule effect, produced by the electric current circulating through the conductors, it is considered that this is divided into equal amounts for each source, that is, for each section of conductor.

So, in total, have:

$Q_1=Q_1^{rec.}+Q_\lambda^{conduction}$-$1/2Q_{Joule}$: from the hot source;

$Q_2=Q_2^{dis.}+Q_\lambda^{conduction}$+$1/2Q_{Joule}$: from the cold source;

and the efficiency of the TEG is:

$$\eta_t = \frac{L_{cycle}}{Q_1} = \frac{I^2Rt}{Q_1^{rec.}+Q_\lambda^{conduction}-\frac{1}{2}Q_{Joule}}$$

and if $Q_\lambda^{conduction}=0$ and $Q_{Joule}=0$ then $L_{cycle}=\alpha(T_1-T_2)It$, $Q_1=\alpha T_1 It$ and then:

$$\eta_t^{\text{Zero losses}} = \frac{L_{cycle}}{Q_1} = \frac{\alpha(T_1-T_2)It}{\alpha T_1 It} = \frac{T_1-T_2}{T_1} = 1-\frac{T_2}{T_1}$$

therefor that is the efficiency of a Carnot cycle, where T_2 is the temperature of the cold source and T_1 is the temperature of the hot source. This is the ideal situation in which the heat conduction and heat losses as Joule effect through the conductors are not taken into account.

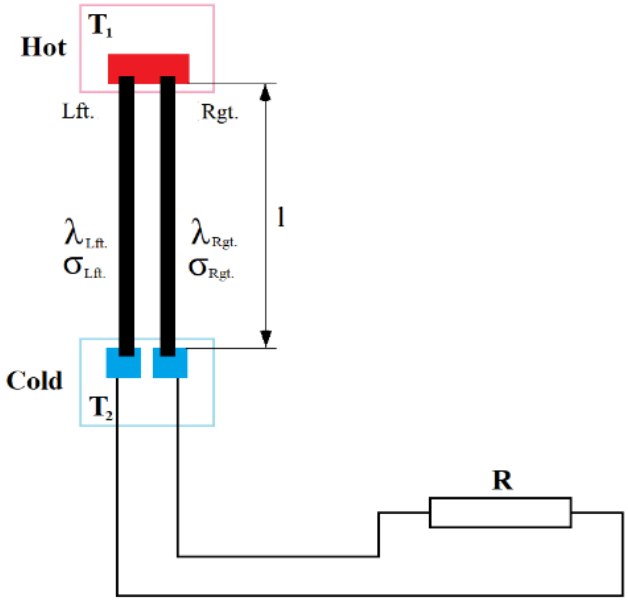

Figure 9. Seebeck element layout

If I take account of these losses, I will have:

$$P_\lambda^{conduction}t=Q_\lambda^{conduction}=\frac{\lambda_{lft.}\sigma_{lft.}-\lambda_{rgt.}\sigma_{rgt.}}{l}(T_1-T_2)\,t=\Psi(T_1-T_2)\,t$$

where $P_\lambda^{conduction}$, is the power transmitted through conduction, $\Psi=\frac{\lambda_{lft.}\sigma_{lft.}-\lambda_{rgt.}\sigma_{rgt.}}{l}$, and σ is the cross-section of the left and right side conductors and λ is the thermal conductivity of the left and right side conductors (Figure 9).

$$P_{Joule}t=Q_{Joule}=I^2rt$$

where $r=\left(\frac{\rho_{lft.}}{\sigma_{lft.}}+\frac{\rho_{rgt.}}{\sigma_{rgt.}}\right)l$, and P_{Joule} is the power lost as Joule effect, and ρ is the resistivity of the conductors on the left and right side. If $\gamma=\frac{R}{r}$, I will have:

$$I=\frac{\alpha(T_1-T_2)}{r+R}=\frac{\alpha(T_1-T_2)}{r(1+\gamma)};\ Q_1^{rec.}=\frac{\alpha^2T_1(T_1-T_2)t}{r(1+\gamma)};\ L_{cycle}=\frac{\alpha^2(T_1-T_2)^2\gamma t}{r(1+\gamma)^2};\ Q_{Joule}=\frac{\alpha^2(T_1-T_2)^2t}{r(1+\gamma)^2}$$

and then,

$$\eta_t=\frac{\frac{\alpha^2(T_1-T_2)^2\gamma t}{r(1+\gamma)^2}}{\frac{\alpha^2T_1(T_1-T_2)t}{r(1+\gamma)}+\Psi t(T_1-T_2)-\frac{1}{2}\frac{\alpha^2(T_1-T_2)^2t}{r(1+\gamma)^2}}=\frac{\frac{T_1-T_2}{T_1}}{1+\frac{\Psi r}{\alpha^2}\frac{(1+\gamma)^2}{T_1\gamma}+\frac{1}{2}\frac{T_1+T_2}{T_1\gamma}}=$$

$$\eta_t^{Carnot}\frac{1}{1+\frac{\Psi_r}{\alpha^2}\frac{(1+\gamma)^2}{T_1\gamma}+\frac{1}{2}\frac{T_1+T_2}{T_1\gamma}}$$

where: $z=\frac{\alpha^2}{\Psi_r}$ is A.F. Ioffe coefficient $z=\frac{\alpha^2}{\lambda_{lft.}\rho_{lft.}+\lambda_{rgt.}\rho_{rgt.}\frac{\sigma_{rgt.}}{\sigma_{lft.}}+\lambda_{lft.}\rho_{rgt.}\frac{\sigma_{lft.}}{\sigma_{rgt.}}+\lambda_{rgt.}\rho_{rgt.}}$, and:

η_t is maximum when z is maximum (or $1/z\rightarrow$ is minimum) but z depends on α, $\lambda_{lft./rgt.}$ which are the thermal conductivity coefficients and $\rho_{lft./rgt.}$ the resistivity of the conductors but also on $\left(\frac{\sigma_{lft.}}{\sigma_{rgt.}}\right)$ the ratio of the conductor sections, that is:

$$z'\left(\frac{\sigma_{lft.}}{\sigma_{rgt.}}\right)=0 \text{ when } \left(\frac{\sigma_{lft.}}{\sigma_{rgt.}}\right)_{(for\ z=max.)}=\sqrt{\lambda_{rgt.}\frac{\lambda_{rgt.}\rho_{lft.}}{\lambda_{lft.}\rho_{rgt.}}} \text{ and}$$

$$z_{max.}=\left(\frac{\alpha}{\sqrt{\lambda_{lft.}\rho_{rgt.}}+\sqrt{\lambda_{lft.}\rho_{rgt.}}}\right)^2$$

and for $\lambda_{rgt.}=\lambda_{lft.}=\lambda$ and $\rho_{rgt.}=\rho_{lft.}=\rho$ thus

$$z_{max.}=\frac{\alpha^2}{4\lambda\rho} \tag{5}$$

Similar for η_t=maximum with respect to γ, denoted by $\gamma_{max.}$, where:

$$\gamma_{max.}=\sqrt{z\frac{T_1+T_2}{2}+1}\,, \tag{6}$$

and $\eta_t=\eta_t^{Carnot}\frac{1}{1+\frac{2(1+\gamma_{max.})}{zT_1}}$ or for z according to $\gamma_{max.}$ will have:

$$\eta_t=\eta_t^{Carnot}\frac{\gamma_{max.}-1}{\gamma_{max.}+\frac{T_2}{T_1}} \tag{7}$$

{and for $Q_{Joule}\approx 0$ I will have $\eta_t=\eta_t^{Carnot}\frac{\gamma'_{max.}-1}{\gamma'_{max.}+1}$ where $\gamma'_{max.}=\sqrt{1+z_{max.}T_1}$ }

If I make a comparative analysis of the three systems for converting thermal energy directly into electrical energy presented above, the conclusion drawn is that a Seebeck-type bridge thermoelectric converter is the best option, both from the point of view of costs and from the point of view of its applicability in aviation.

Thus, bridges with low operating temperatures, between 200^0C and 1000^0C, which are currently mass-produced, can be used. Even if these Seebeck bridges have low transfer efficiencies (between 5% and 30%), considering that they are used to recover heat that is lost by conduction through the walls of the jet engine to the outside, they can be used as a cooling and insulating option for these surfaces. For the heat exchange carried out in the gas flow after the combustion chamber, with the role of replacing the gas turbine, materials that allow high operating temperatures, from 1500^0C to 2500^0C, and with higher efficiencies, of about 30% are suitable. For this reason, I will present such materials, respectively, thermocouples material, in the next chapter.

6 Seebeck Materials [18, 19], [23–27], [30, 31, 33, 34]

For mass-produced Seebeck bridges, the materials used are semiconductor metals alloyed and doped to form p- or n-type junctions. The semiconductor materials can be used up to maximum temperatures of approximately 250^0C. These can use an alloy of Germanium and Silicon, the first types of such bridges manufactured. Other types of generators can use alloys of Bismuth, Antimony and Tellurium, such as $(BiSb)_2Te_3$ and $Bi_2(TeSe)_3$.

Germanium-Tellurium and Lead-Tellurium alloys can also be used. Newer research also uses other alloys, in which metals are used, as follows, but not limited to: Fe, Cs, Ca, Ce, Mn, Sn, Co, Ce, Ag, La, Nd, S, C, all of these alloys greatly improving the performance of these generators.

For high temperatures, typical for the gas temperature of jet engines of this type, combinations of Nickel, Chromium, Silicon, Magnesium, Aluminum, Manganese can be used for temperatures up to 1200^0C, Platinum-Rhodium alloys for temperatures between 1500^0C and 1700^0C and Tungsten (Wolfram)-Rhenium for temperatures above 2300^0C [20] basically used for pyrometer technology. These last thermocouples can be used to recover energy from the gas flow after the combustion chamber, but their thermoelectric figure of merit is extremely low, making them unsuitable for efficient power generation compared to pyrometry. For actual energy recovery, advanced thermoelectric materials with a higher figure of merit (ZT) are required. For example, oxyselenides (BiCuSeO) can achieve a ZT of approximately 1.4 at 800 K, and SnSeS compounds have been reported to reach a ZT of 3.07 at 700 K [30], while radioisotope thermoelectric generator materials can operate up to 1200 K. However, due to high costs and material limitations, metal-based high-temperature thermocouples remain restricted to pyrometer technology or specialized space applications. Recent research has used oxide-based materials for such generators, with operating temperatures comparable to those of high-melting-point metals.

7 Current cases of thermoelectric converters use

Apart from the use in ground heat recovery installations, in thermoelectric power plants or industrial installations that release residual substance at high temperature, in which case magneto-hydro-dynamic generators can be used with good efficiency, I have found such systems, mainly Seebeck-type thermoelectric systems in the automotive sector [29, 32].

These systems recover between 330W and 1000W on automobile, reaching values of 3000W to 5000W on truck train and vessel engines. The efficiencies of these systems, due to the lower operating temperatures, are between 10% and 30%. (ref.: [17] Automotive Thermoelectric Generators and HVAC, John Fairbanks, US Department of Energy).

8 Experiment on turbo-shaft jet engine

I will make a numerical estimation for a Seebeck thermocouple of materials that I will use in the experimental verification presented in the following chapter corresponding to the generator used in the experimental part. For numerical calculation I used formulas (5), (6) and (7) presented in Subsection 5.3. I will consider a parameter z between 0 and $5 \cdot 10^{-3} K^{-1}$, and the estimated temperature differences will be between 0 and 260^0K, potential differences to be obtained with thermocouples in which materials with operating temperatures above 2300^0C were used, and at external temperatures typical of the stratosphere. I mention these generators that operate at lower temperatures can also be used to recover the heat lost by the engine through the housings of components with lower temperatures, but suitable for energy recovery as heat.

With these data, after performing the calculations I present the values in Table 4, represented graphically in Figure 10:

z	$\eta_{t=}$	$\gamma_{max.=}$	
t2(cold)=	200	t1(hot)=:	2600
0.00	0	1	
1.00	0.3118	1.5492	
2.00	0.4325	1.9494	
3.00	0.5014	2.2804	
4.00	0.5474	2.5690	
5.00	0.5809	2.8284	
t2(cold)=	200	t1(hot)=:	1100
0.00	0.0000	1.0000	
1.00	0.1588	1.2845	
2.00	0.2489	1.5166	
3.00	0.3091	1.7176	
4.00	0.3531	1.8974	
5.00	0.3872	2.0616	
t2(cold)=	200	t1(hot)=:	400
0.00	0.0000	1.0000	
1.00	0.0427	1.1402	
2.00	0.0750	1.2649	
3.00	0.1007	1.3784	
4.00	0.1218	1.4832	
5.00	0.1396	1.5811	

Table 4. TEG parameters values

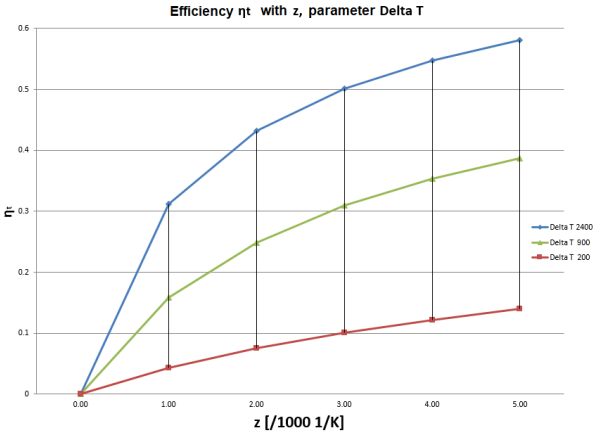

Figure 10. Efficiency η_t with z, parameter ΔT

9 Experimental Verification and Estimation of Energy Generation from Residual Heat Flown on a Turbo-Shaft Jet Engine

To estimate the power lost through the outer walls of a jet engine, I used a Titan Gas Turbine T-62T-32 turbo-shaft jet engine, manufactured by the SOLAR Division of International Harvester Company, San Diego, California, a turbo-shaft jet engine that is used for military technology (APU: Auxiliary Power Unit, for various types of military helicopters) or on ground applications, such as ground generators (GPU: Ground Power Unit, used by the US Navy and USAF). The turbo-axial jet engine on which we conducted the experiment is used to power an ultralight helicopter, according to the identification plate (Figure 13, image on the helicopter). Here are some photos of this turbo-shaft jet engine (Figures 11 and 12, obtained with the support of: "SOLAR Division of International Harvester Company, San Diego, California"):

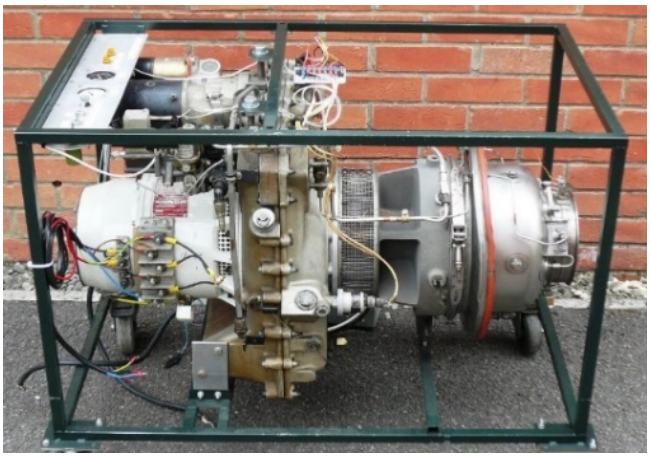

Figure 11. Turbo-shaft jet engine Solar installed on a GPU

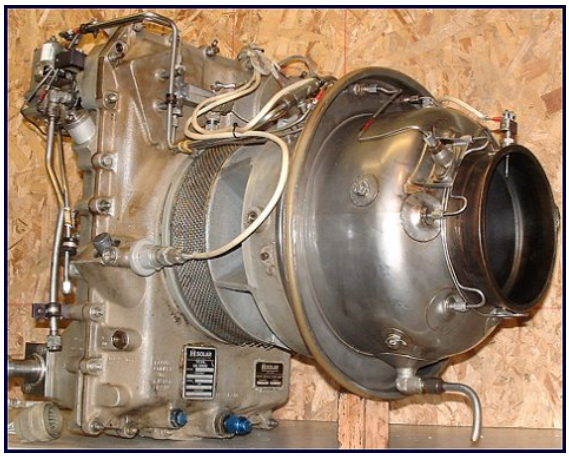

Figure 12. View of a Solar turbo-shaft jet engine

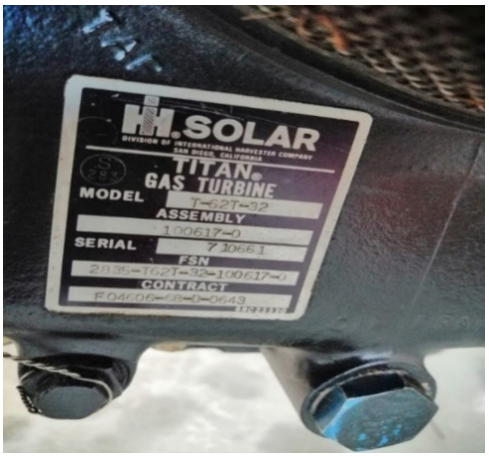

Figure 13. Identification plate of Solar turbo-shaft jet engine

Following the measurements, the temperature on the ”hot” metal part of the exhaust diffuser was 158^0C on the ”hot” side at 40% of power, and approximately 50^0C on the ”cold” side, at the same engine load. At maximum engine power, on the hot side I measured 222^0C on the ”hot” side and a temperature of approximately 50^0C on the ”cold” side. I mention that the gases in the exhaust flow have a temperature of 362^0C at a 40% power load and 567^0C at a maximum power of 100%. I also mention that the external temperature at the time of measurement was 26^0C and the atmospheric pressure at the runway level was 1011hPa. The engine's thermal load was with stabilized parameters (the helicopter at takeoff parameters).

Below I present some photos (Figures 14 and 15) that confirm the above data:

Figure 14. Hot case temperature for 100% power

Figure 15. Hot case temperature for 40% power

To estimate the power generated I will use Eureca Seebeck thermoelectric generators, manufactured by Messtechnic GmbH, type TEG2-50-50-40/200, which have a maximum power of 40W and a maximum operating temperature of 200^0C, have dimensions of 50mm x 50mm x 3.3mm thickness and a weight of 38 grames.

This is manufactured with a Bi_2Te_3-PbTe thermocouple, whose Ioffa coefficient is z=0.5·10-3K-1, according to the generator's data sheet [16], the thermoelectric potential (electric force) is 0.0516 V/K, the internal resistance is 0.673Ω, and the thermal conductivity of the plate is γ=1.90W/K.

For the experiment, I simulated the temperature of the turbo-shaft jet engine using an electrical resistance (smooth iron resistance) that I adjusted to heat up to a temperature of approximately 150^0C (so as not to destroy the Seebeck generator).

I measured the electrical parameters of the generated electrical energy that supplies a consumer (20W/6V light bulb) of 20W, slightly higher than the maximum power generated by the Seebeck generator.

According to the Eureca graph for Seebeck bridge used (courtesy: www.eureca.de) for temperature differences ΔT with values of 200^0C, 100^0C and 50^0C, graphically represented in Figure 16 shown below:

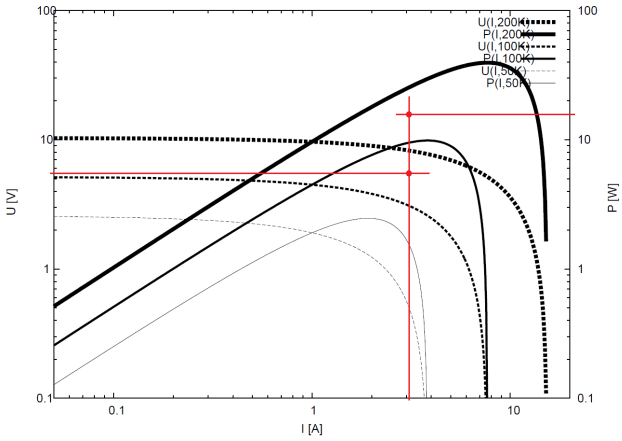

Figure 16. Equilibrium points for Eureca Seebeck bridge for Voltage and Power with Current

From Eureca data sheet in [16], the values for the Seebeck generator used are:

$\alpha = 0{,}0516$ V/K;

$\rho = 0{,}673\ \Omega$;

$\lambda = 1{,}90$ W/K.

Following the experiment carried out to simulate energy recovery from the hot zone of the turbo-shaft jet engine, the following were measured, at a temperature stabilized at 154.0^0C: U=5.33V, I=3.56A for which P=18.98W results, and after approximately 2 minutes from making contact with the electrical resistance of the Seebeck generator, the generated electric current decreased to I=3.01A for which P=16.04W and it was stabilized.

I mention when the parameters are stabilized after a decrease in the generated power of approximately 15.49%. The experiment lasted 10 minutes.

It is important to discuss the limitations of this laboratory simulation and how real-world environmental factors would affect the Seebeck generators in a practical helicopter or aircraft installation. In initial tests, attempting to mount the Seebeck modules directly onto the hot components of the turbo-shaft engine resulted in the destruction of two modules. This was caused by the lack of precise temperature control during startup and transient power settings. To prevent further damage to the COTS (Commercial Off-The-Shelf) modules, a controlled electrical resistance simulation was adopted instead. In an operational environment, high-velocity convective airflow over the engine casing would alter the boundary layers and temperature gradients, which are critical to the thermoelectric performance. Additionally, mechanical vibrations and thermal shock cycles during engine start/stop cycles could degrade the thermal contact resistance and mechanical attachment of the modules. For a production-ready aviation system, high-temperature thermoelectric materials capable of withstanding thermal shocks and uncontrolled temperature excursions must be used. Adequate mechanical fastening and thermal interface materials can mitigate contact degradation from vibration. Compared to classic gas turbines that operate under severe rotational stress and have operational lifespans of a few thousand hours, static Seebeck modules face much milder stress profiles, offering lower manufacturing and maintenance costs, with expected lifespans extending to hundreds of thousands of hours.

Below are some photos from the experiment (Figures 17, 18, 19 and 20):

Figure 17. Simulated temperature

Figure 18. TEG voltage

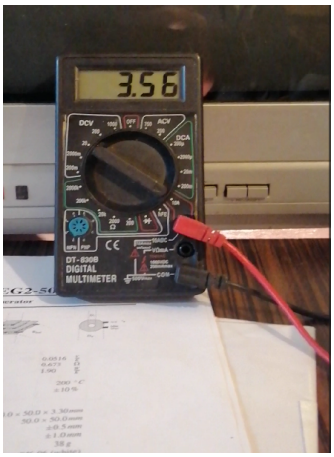

Figure 19. Initial current

Figure 20. Stabilized current

10 Conclusions and interpretation of experimental results

I have chosen this verification option because it would not have been technically possible to perform the verification on the turbo-shaft engine, first of all because the turbo-shaft is mounted on an ultralight helicopter, and at the maximum speed of the turbo-shaft engine, the Seebeck generator could be destroyed.

Thus, for a ground operating mode of the turbo-shaft engine at 40% of the maximum power, the temperature measured by me on the hot side is 158^0C, and the power is 44.0 kW.

The estimation of the power generated on a diameter of 54.293 cm (according to the technical sheet of the turbo-shaft) will be:
Perimeter: 54.293 x 3.141592 = 170.566 cm, on which 170.566: 5 = 34 pieces Seebeck plates can be mounted.
For the length of the hot side of approximately 50 cm, 340 Seebeck plates could be mounted, which will generate:
340 x 16.04 W = 5.454 kW.

This power of 5.454 kW represents 12.40% of the useful mechanical shaft power of the engine at that speed (44.0 kW). Since casing heat and exhaust represent waste thermal energy, it is more rigorous to evaluate this recovery relative to the total chemical energy input of the fuel. Assuming a typical thermal efficiency of approximately 20% for this class of turbo-shaft engine, the total chemical energy input rate of the fuel is approximately 220.0 kW (44.0 kW / 0.20). Thus, the recovered electrical power of 5.454 kW represents approximately 2.48% of the total chemical energy input of the fuel (5.454 kW / 220.0 kW). Given that approximately 80% of the fuel's energy is lost as waste heat to the cold source (exhaust gas and engine walls), this casing recovery represents a retrieval of approximately 3.1% of the total waste thermal energy. This recovered energy is a direct gain from the casing walls, which would otherwise be lost to the environment in a standard gas turbine, and can be used to recharge the on-board batteries or drive the electric compressor. I cannot recover the energy from exhaust gases which is also a lost energy because I do not have Seebeck bridges suitable for this temperature.

REFERENCES

[1] C. Berbente, N. V. Constantinescu, *Dinamica gazelor, Partea I*, Centrul de multiplicare cursuri I.P.B., București, Romania, 1985.

[2] E. Carafoli, V. N. Constantinescu, *Dinamica fluidelor incompresibile*, Editura academiei R.S.R., București, Romania, 1981.

[3] E. Carafoli, V. N. Constantinescu, *Dinamica fluidelor compresibile*, Editura academiei R.S.R., București, Romania, 1984.

[4] E. Carafoli, V. N. Constantinescu, *Dinamica fluidelor viscoase în regim laminar*, Editura academiei R.S.R., București, Romania, 1987.

[5] V. N. Constantinescu, St. Găletușe, *Mecanica fluidelor și elemente de aerodinamică*, Editura didactică și pedagogică, București, Romania, 1983.

[6] M. Marinescu, Instalaţii de ardere, culegere de probleme, Editura tehnică, București, Romania, 1985.

[7] V. Pimsner, *Mașini cu palete, procese și caracteristici*, Editura tehnică, București, Romania, 1988.

[8] V. Pimsner, *Motoare aeroreactoare*, Vol. **1**, Editura didactică și pedagogică, București, Romania, 1983.

[9] V. Pimsner, ș.a., *Procese în mașini termice cu palete, aplicaţii și probleme*, Editura tehnică, București, Romania, 1986

[10] V. Pimsner, ș.a., *Termodinamica tehnică, culegere de probleme*, Editura didactică și pedagogică, București, Romania, 1982.

[11] V. Stanciu, *Modelarea tracţiunii sistemelor de propulsie*, Editura Urania, ISBN 973-85530-0-8, București, Romania, 2001.

[12] M. Tomescu, *Proprietăţile combustibililor și lubrifianţilor pentru motoarele de aviaţie*, Editura tehnică, București, Romania, 1985.

[13] V. Stanciu, G. Cican, *Simularea performanţelor turbomotoarelor de aviaţie în FORTRAN*, Editura Printech, ISBN 978-606-23-0310-5, București, Romania, 2015.

[14] Alejandro Millán-Merino, Pierre Boivin. *A new single-step mechanism for hydrogen combustion. Combustion and Flame*, 2024, 268, pp.113641. 10.1016/j.combustflame.2024.113641. hal-04943874

[15] V. A. Kirillin, *Termodinamica*, Editura ştiinţifică și enciclopedică, București, Romania, 1985.

[16] * * * http//:www.eureca.de, Catalog.

[17] * * * Automotive Thermoelectric Generators and HVAC, John Fairbanks, US Department of Energy, 2013 Annual Merit Review and Peer Meeting DOE Vehicle Technologies Office, Washington DC, May 17, 2013.

[18] G. J. Snyder, E. S. Toberer, *Complex Thermoelectric Materials*, Nature materials, https://en.wikipedia.org/wiki/Doi_(identifier):https://doi.org/10.1038%2Fnmat2090. https://en.wikipedia.org/wiki/PMID_(identifier) https://pubmed.ncbi.nlm.nih.gov/18219332, 2008.

[19] G. S. Nolas, J. Sharp, H. J. Goldsmid, *http://link.springer.com/10.1007/978-3-662-04569-5,* Springer Series in Materials Science, Vol. **4**, Berlin, Heidelberg: Springer- Verlag Berlin Heidelberg New York. https://en.wikipedia.org/wiki/Doi_(identifier):https://doi.org/10.1007%2F978-3-662-04569-5. https://en.wikipedia.org/wiki/ISBN_(identifier) https://en.wikipedia.org/wiki/Special:BookSources/3-540-41245-X, 2001.

[20] * * * http//:www.pyromation.com, Thermocouple Material Specifications.

[21] S. Nutu, *Electro-jet engine: a jet engine without turbine - Part 1: Presentation of electro-jet engine,* INCAS BULLETIN, Vol. 17 Issue 4, October-December 2025, Bucharest, DOI: 10.13111/2066-8201.2025.17.4.10, ISSN2066-8201

[22] S. Nutu, *Electro-jet engine: a jet engine without turbine - Part 2: Electric power generation,* INCAS BULLETIN, Vol. 17 Issue 4, October-December 2025, Bucharest, DOI: 10.13111/2066-8201.2025.17.4.11, ISSN2066-8201

[23] *** NBS Monograph 40, U.S. Department of Commerce, Thermocouple Materials;

[24] *** Englehard Industries, Inc., K-76 Technical Reference, Other Types of Thermocouples;

[25] *** Barbara Hudson, JMS Southeast, Inc., Type M and K Thermocouples;

[26] *** https://tecteg.com Tellurex, Inc., TEG-Seebeck Technology;

[27] *** Jeffrey G. Snyder, Eric S. Toberer, Complex Thermoelectric Materials;

[28] *** https://www.prattwhitney.com P&W Canada RTX Corp. United Technologies.

[29] Prakash, Om & Kashyap, Ishan & Kumar, Ayush & Bhushan, Bharath & Kumar, Anil & Chauhan, Prashant. (2021). Automobile based heat energy recovery systems. WEENTECH Proceedings in Energy. 11-23. 10.32438/WPE.022021.

[30] Wang, J.; Yin, Y.; Che, C.; Cui, M. Research Progress of Thermoelectric Materials—A Review. *Energies* **2025**, *18*, 2122. https://doi.org/10.3390/en18082122

[31] G, Krupanidhi & A, Ramya & B, Sowmya. (2022). Thermoelectric Generators and the Seebeck Effect. World Journal of Advanced Research and Reviews. 16. 1448-1455. 10.30574/wjarr.2022.16.3.1409.

[32] Andrew Royale, Milan Simic, Research in Vehicles With Thermal Energy Recovery Systems, Procedia Computer Science, Volume 60, 2015, Pages 1443-1452, ISSN 1877-0509, https://doi.org/10.1016/j.procs.2015.08.221.

[33] Jin-Cheng Zheng, Recent advances on thermoelectric materials Front. Phys. China, 2008, 3(3): 269-279

[34] Clotilde Boulanger, Thermoelectric Material Electroplating: a Historical Review, Journal of ELECTRONIC MATERIALS, Vol. 39, No. 9, 2010, DOI: 10.1007/s11664-010-1079-6

[35] John Davison, Energy Consultant, Cheltenham, Glos., UK, A review of gas turbines and their ability to use hydrogen containing fuel gas, Report for Energy Technologies Institute September 2016

[36] Salehi, Vahid Douzloo, Munich University of Applied Sciences, International conference on engineering design, Application of a holistic approach of hydrogen internal combustion engine (hice) busses, 16-20 August 2021, Gothenburg, Sweden

[37] Giacomazzi, E.; Troiani, G.; Di Nardo, A.; Calchetti, G.; Cecere, D.; Messina, G.; Carpenella, S., Hydrogen Combustion: Features and Barriers to Its Exploitation in the Energy Transition. Energies 2023, 16, 7174. https://doi.org/10.3390/en16207174